THESIS FOR THE DEGREE OF LICENTIATE OF ENGINEERING

Hydrogen Production by Integration of Fluidized Bed Heat Exchanger in Steam Reforming of Natural Gas

VIKTOR STENBERG

Department of Space, Earth and Environment
CHALMERS UNIVERSITY OF TECHNOLOGY
Gothenburg, Sweden 2019

Hydrogen Production by Integration of Fluidized Bed Heat Exchanger in Steam Reforming of Natural Gas

VIKTOR STENBERG

©VIKTOR STENBERG, 2019.

Department of Space, Earth and Environment
Chalmers University of Technology
SE-412 96 Gothenburg
Sweden
Telephone + 46 (0) 31 772 1000

Chalmers Reproservice
Gothenburg, Sweden 2019

Hydrogen Production by Integration of Fluidized Bed Heat Exchanger in Steam Reforming of Natural Gas

VIKTOR STENBERG
Division of Energy Technology
Department of Space, Earth and Environment
Chalmers University of Technology
SE-412 96 Gothenburg, Sweden

Abstract

The possibility to integrate fluidized beds as heat sources for steam reforming in hydrogen production plants is examined in this work. Sites with large-scale production and consumption of hydrogen such as refineries are considered as especially interesting. The proposed processes include the traditional catalytic steam reforming of natural gas (SMR), shift reactors and purification steps; the main difference is the reformer furnace. In the conventional plant a gas-fired furnace is utilized where the heat necessary for the endothermic steam reforming reaction is generated and transferred to the steam reforming tubes mainly by radiation. The alternative which is investigated in this work is to immerse the reformer tubes in fluidized bed heat exchangers. Based on the high heat transfer which can be expected from a bubbling fluidized bed to an immersed tube surface, the potential benefits are significant compared to conventional technology mainly as a result of improved heat transfer to the reformer tube. The proposed processes are compared with conventional steam methane reforming from thermodynamic, economic and environmental point of view. The work combines process simulations of hydrogen production plants using Aspen Plus with lab-scale experiments on fluidized bed combustion and fluidized bed heat transfer.

The first proposed process uses oxygen carrier particles in a single fluidized bed heat exchanger where the fuel is converted in the bed; this is a novel process facilitated by the use of oxygen carrier particles. The process is estimated to reduce the supplementary fuel consumption of natural gas which thereby causes the reduction of CO_2 emissions from the process by approximately 12% and the levelized hydrogen production cost is approximately 7% lower in comparison with the conventional SMR plant. Lab-scale experiments were performed with an inert silica sand and an oxygen carrier ilmenite as bed materials using methane as fuel, the component in the fuel gas which is considered to be the most difficult to convert. The experiments showed that methane was converted in the dense bed even at moderate furnace temperatures (i.e., 600-800˚C) and the use of ilmenite increased the fuel conversion in the bed.

The second proposed process is based on integration of SMR with chemical-looping combustion where an oxygen carrier is circulated between two interconnected fluidized bed reactors. In the air reactor, the oxygen carrier is oxidized with air and in the fuel reactor, the oxygen carrier is reduced by the fuel. The flue gas stream obtained from the fuel reactor is not diluted with N_2 and the CO_2 produced can easily be captured. The supplementary fuel consumption increases only slightly

compared to the first proposed process. The energy penalty to enable CO_2 capture is small and the supplementary fuel consumption is still significantly lower than for the conventional process.

The third proposed process is also based on chemical-looping combustion but uses biomass instead of natural gas as supplementary fuel, which enables the possibility of achieving net negative emissions from the hydrogen production process. By using a higher steam-to-carbon ratio and a higher temperature at the outlet of the reformer, it is possible to increase the hydrogen yield in the process and achieve significant negative emissions from the process.

One of the key reasons for using fluidized beds as a heat source is that the heat transfer from bed to tube is expected to be higher than that in the conventional furnace. Although much work in literature has been done to investigate bed-to-tube heat transfer, most of the reported experiments have been conducted at bed temperatures lower than 400˚C which is below the operating temperature of the relevant processes. In this work, lab-scale experiments were therefore performed to verify if: i) high bed-to-tube heat transfer coefficients can be obtained in the targeted systems; and ii) well-known heat transfer correlations determined at lower temperatures can also be used to predict the heat transfer at higher bed temperatures. The estimated heat transfer coefficients were high, i.e., 768-1858 W/(m^2K) at 400-950˚C bed temperature, for the tested bed materials of relevant particle sizes. Three of the heat transfer correlations studied showed good accuracy to predict the bed-to-tube heat transfer coefficient in the experimental unit. The heat transfer correlations could therefore be used to predict the bed-to-tube heat transfer coefficient for the three proposed process configurations. Both experimental campaigns supported the claim that fluidized bed heat exchangers are suitable for use in the proposed SMR application. The proposed processes display high thermal efficiency and the possibility to achieve significant reductions in CO_2 emissions in the industry of hydrogen production. All three proposed processes are considered as interesting for large-scale plants which could provide several environmental benefits and this work could be used as a support for industrial implementation.

List of publications included in the thesis

I. Stenberg V, Rydén M, Mattisson T, Lyngfelt A. Exploring novel hydrogen production processes by integration of steam methane reforming with chemical-looping combustion (CLC-SMR) and oxygen carrier aided combustion (OCAC-SMR). International Journal of Greenhouse Gas Control. 2018;74:28-39.

II. Stenberg V, Spallina V, Mattisson T, Rydén M. Techno-economic analysis of H_2 production processes using fluidized bed heat exchangers with steam reforming – Part 1: Oxygen carrier aided combustion. 2019. Submitted for publication in International Journal of Hydrogen Energy.

III. Stenberg V, Rydén M, Mattisson T, Lyngfelt A. Combustion of Methane in Bubbling Fluidized Bed with Oxygen Carrier Aided Combustion (OCAC), 23rd International Conference on Fluidized Bed Conversion, Seoul, Korea, May 13-17, 2018.

IV. Stenberg V, Sköldberg V, Öhrby L, Rydén M. Evaluation of bed-to-tube surface heat transfer coefficient for a horizontal tube in bubbling fluidized bed at high temperature. Powder Technology. 2019. Accepted manuscript.

Author contribution

Viktor Stenberg is the principal author of Papers I–IV. Professor Tobias Mattisson contributed with discussion and editing of Papers I-III. Professor Anders Lyngfelt contributed to discussion of Papers I and III as well as editing of Papers I. Dr Vincenzo Spallina contributed to develop the Aspen Plus simulation model in Paper II as well as discussion and editing of this paper.

M.Sc Lovisa Öhrby contributed to the experimental work of Paper IV. M.Sc Viktor Sköldberg contributed to the experimental work, discussion and editing of Paper IV. Associate Professor Magnus Rydén contributed ideas, discussion, and editorial support for all four papers.

List of publications not included in the thesis

I. Stenberg V, Rydén M, Mattisson T, Lyngfelt A. Hydrogen production by integration of steam reformation with chemical-looping combustion, 4th International Conference on Chemical Looping, September 26-28, 2016, Nanjing, China.

II. Aronsson J, Krymarys E, Stenberg V, Mattisson T, Lyngfelt A, Rydén M. Improved Gas-Solids Mass Transfer in Fluidized Beds – Confined Fluidization in CLC. Energy & Fuels. 2019. Accepted manuscript.

Acknowledgements

I have always sought challenges which I myself and others around me consider to be difficult for me to succeed with. Pursuing a PhD is one of those challenges. You are many who makes it possible for me to take on this adventure and this section is an opportunity for me to recognize these people. I am able to experience this PhD adventure thanks to supports from amazing people whom I have met along my journey.

First of all, I want to thank those involved at the division of Energy Technology at Chalmers. I am very thankful to my main supervisor Magnus Rydén who has been a great support both when things go well to discuss plans for future work but perhaps even more so when you are able to calm me down when things do not go as well. I would also like to thank Tobias Mattisson and Anders Lyngfelt for interesting discussions and most valuable input. Henrik Leion should also be recognized for being the one which gave me the opportunity to pursue a master thesis within the world of oxygen carriers which led me into this research group in the end. I would also like to thank Rustan Hvitt, Jessica Bohwalli and Ulf Stenman for helping me setting up the experimental activities in the new reactor system. I have learned a lot from discussing with you and it has been most valuable when planning my experimental work. Every single colleague at Energy technology should be thanked for contributing to a fantastic working environment. I have had so many interesting discussions with you both unrelated and related to work which I have enjoyed very much, I'm looking forward to spending more time with you in my future work. A special thanks to Holger for being a great office roommate whom I have shared both laughs, kombucha brewing and interesting discussions with the last two years or so.

Secondly, I would also like to send some well-deserved thanks to some people outside of Sweden who has been involved in this work. I am happy for the interesting discussions I have shared with Martin Østberg, Morten Boberg Larsen and Francois-Xavier Chiron at Haldor Topsøe during our project meetings. I am most thankful to Vincenzo Spallina for providing the opportunity to conduct some of my PhD in the Netherlands with the research group of Chemical Process Intensification at the Technical University of Eindhoven. I also want to thank the rest of the research group at TU/e for making my stay in Eindhoven so stimulating!

Working on this research topic has allowed me to work with many different research areas and there are so many of you which have contributed to this work indirectly through discussions with me on various topics, thus the notion "none mentioned, none forgotten" applies very much. Outside of the research community but not less important I want to thank my family and friends for supporting me to pursue both with my ambitions at and outside of work. This gives me great joy in what I am doing and is invaluable to my personal journey in life.

This work has been supported by the Swedish Energy Agency (project 40559-1 - Heat to endothermic industrial processes with new efficient combustion method in fluidized bed).

Viktor Stenberg

Gothenburg, May 2019

Table of contents

LIST OF PUBLICATIONS INCLUDED IN THE THESIS III

LIST OF PUBLICATIONS NOT INCLUDED IN THE THESIS V

ACKNOWLEDGEMENTS VII

TABLE OF CONTENTS IX

1. INTRODUCTION 1

2. BACKGROUND 5

2.1. Steam Methane reforming 5

2.2. Chemical-looping combustion 5

2.3. Oxygen carrier aided combustion 6

2.4. Fluidized bed heat exchanger 8

3. EXPERIMENTAL SETUP 11

3.1. OCAC reactor 11

3.2. FBHE reactor 13

4. METHODOLOGY 17

4.1. Thermodynamic evaluation of solutions with FBHE integrated with SMR for hydrogen production 17

4.2. Economic evaluation of a single FBHE integrated with SMR for hydrogen production 20

4.3. Experimental investigation of OCAC in BFB 21

4.4. Experimental investigation of bed-to-tube surface heat transfer in FBHE 22

5. RESULTS AND DISCUSSION 25

5.1. Thermodynamic evaluation of solutions with FBHE integrated with SMR for hydrogen production 25

5.2. Economic evaluation of a single FBHE integrated with SMR for hydrogen production 28

5.3. Experimental investigation of OCAC in BFB 30

5.4. Experimental investigation of bed-to-tube surface heat transfer in FBHE 32

6. CONCLUSIONS 37

7. FUTURE WORK 39

ABBREVIATIONS 41

NOMENCLATURE 41

REFERENCES 43

1. Introduction

In the 18th century the industrial revolution began which marked the transition from a society based on agriculture and hand production methods to machine manufacturing. This revolution led to rapid technological, economic and population growth as well as a growth in energy consumption with coal as dominating energy source. During the 20th century a diversification of fossil energy consumption was observed where use of crude oil and natural gas came to play an important role as well. At the same time, the energy demand increased rapidly, leading to an increase in greenhouse gas (GHG) emissions. GHG emissions, where carbon dioxide is the major contributor, has been linked to the increase in average global temperature and climate change. Fossil fuel consumption corresponded to 87% of the global primary energy consumption in 2017 [1]. At the COP21 conference in Paris a recent international agreement was made to target a global warming to well below 2˚C compared to pre-industrial levels and attempt to limit the temperature increase to 1.5˚C. The IPCC special report on a global warming of 1.5˚C discusses the carbon budget to limit the global warming within the 1.5˚C target and virtually all the emission scenarios overshoot a 1.5˚C temperature increase but is compensated by future negative emissions [2]. It is clear that large-scale deployment of negative emissions technologies is required to have a possibility to limit the global warming to 1.5˚C. In order to achieve drastic reductions in CO_2 emissions, significant changes in the energy sector are required.

The chemical industry is part of this sector, and one of the most important chemical products today is hydrogen. Hydrogen is used for production of fertilizers and methanol, in oil refining and metallurgical industries, and also as an energy carrier. The annual hydrogen production corresponds to approximately 2% of the primary energy demand [3, 4]. Approximately 95% of the hydrogen produced today is based on fossil fuels [3] and hydrogen production accounts for more than 1% of the global CO_2 emissions [5], approximately 500 Mton CO_2 per year. Hydrogen production based on fossil fuels is considered to be the most economically feasible alternative during the next 20 years and they could also play an important role in the longer term, i.e. 20-50 years [6]. The two main production routes are steam reforming of methane/natural gas and reforming of oil/naphtha, which account for 48% and 30% of the global hydrogen production, respectively [7]. The two routes are similar processes, the main difference being the fuel used. The rest is produced from coal gasification, 18% and electrolysis, 4% [5]. Large-scale SMR production is recognized as benchmark technology for hydrogen production today based on its general economic feasibility globally [5]. The Compound Annual Growth rate (CAGR) for hydrogen is expected to exceed 6% from 2016 to 2022 [5], mainly driven by legislation to regulate desulfurization of petroleum products and increased demand for hydrogen in the transportation sector. Hydrogen is very interesting as transportation fuel since they can be used in fuel cell vehicles which are quiet, energy efficient and cause zero emissions. The deployment of fuel cell electric vehicles is at present limited (around 7000 vehicles on the roads in 2017 [8]) but this could increase significantly. The Hyundai Motor Group has for example announced that they aim to produce 700 000 fuel-cell systems annually by 2030 which includes 500 000 units for Fuel Cell Electric Vehicles (FCEV) [9].

Another interesting initiative is HYBRIT presented by SSAB, LKAB and Vattenfall which targets to replace coal with hydrogen in the steel-making process [10]. The steel industry is a major contributor to CO_2 emissions both globally, around 7%, and in Sweden, approximately 10%. This is another example of a potential source for increased demand for hydrogen in the future.

Based on foreseen future demand for hydrogen, it is important to target a more sustainable industrial hydrogen production process. As presented above, the most common hydrogen production method is to use steam reforming. The process is commonly based on a reformer, a shift reactor and a hydrogen purification system based on pressure swing adsorption (PSA). The key component in this process is the reformer where steam and hydrocarbons react at high temperature and high pressure in tubes in presence of a catalyst. The steam reforming reaction is endothermic, and the heat required for the reaction is provided by external heating of the tubes in the reformer furnace. The syngas produced in the reformer is fed to a shift reactor where additional hydrogen is produced. This stream is further fed to a PSA unit where a high purity product stream of hydrogen is produced as well as an off-gas containing CO, H_2, CH_4 and CO_2 which is used as fuel gas in the reformer furnace. In addition to the off-gas, supplementary fuel is introduced to the furnace to provide the heat necessary for the steam reforming reaction, see the “Old reformer” in Figure 1.

One approach to achieve that is to find a process which can provide a higher hydrogen production efficiency and therefore reduce the supplementary fuel consumption and the required fossil fuel input to the process per unit of produced hydrogen. The supplementary fuel consumption can for example be reduced by improving the heat transfer to the reformer tubes. In order to improve the heat transfer to the reformer tubes the gas-fired furnace (GFF) could be replaced with a single fluidized bed heat exchanger where the reformer tubes are immersed in the fluidized bed of oxygen carrier particles [11]. The concept is illustrated in Figure 1.

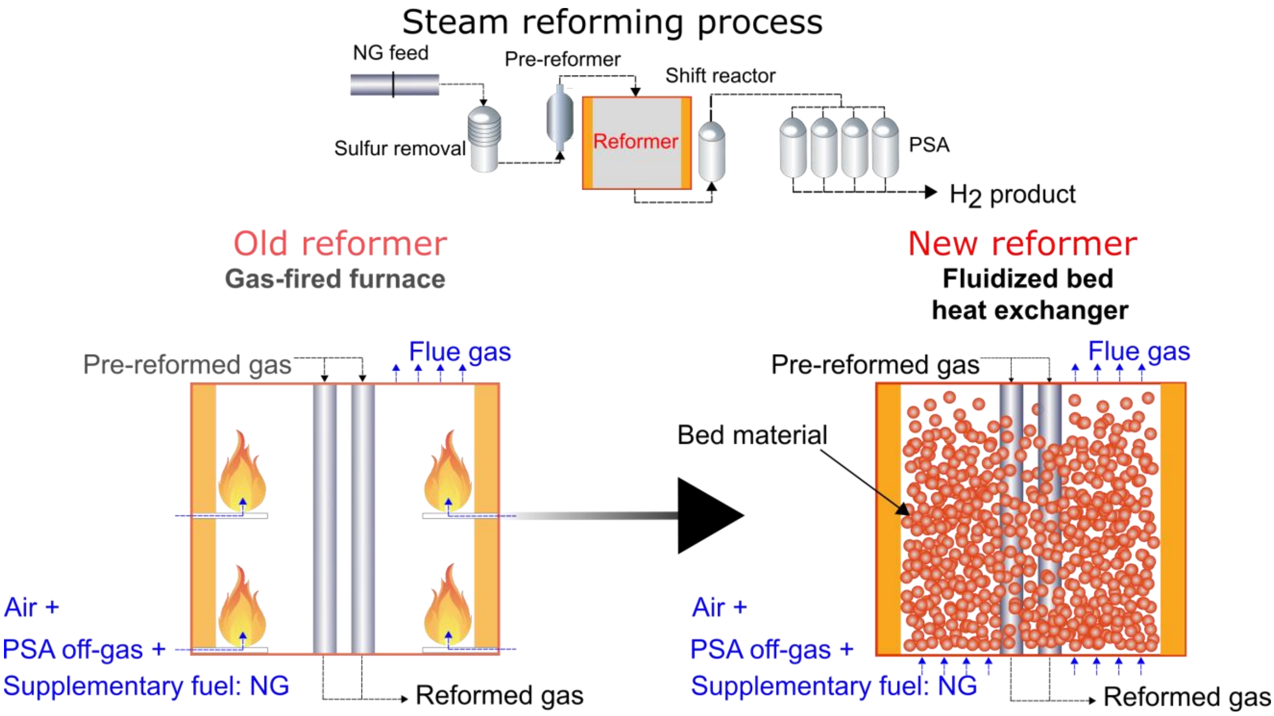
Steam reforming process
NG feed
Pre-reformer
Shift reactor
Sulfur removal
Reformer
PSA
H2 product
Old reformer
Gas-fired furnace
New reformer
Fluidized bed heat exchanger
Pre-reformed gas
Flue gas
Bed material
Air +
PSA off-gas +
Supplementary fuel: NG
Reformed gas

Figure 1. Illustration of the concept to replace the gas-fired furnace with a fluidized bed heat exchanger.

In order to reach close to net zero CO_2 emissions from a plant based on the SMR process with externally heated reformer tubes it could be possible to integrate the process with either post-combustion capture technologies [12] or chemical-looping combustion (CLC) for inherent CO_2 capture [13]. Chemical-looping has been identified as an one of the most promising options to obtain a low incremental cost for CO_2 capture [14]. One of the key reasons for this is that it has a low energy penalty compared to most of the other technologies capture technologies such as post-combustion capture and ideally no cost of CO_2 separation [14]. The option to integrate SMR with CLC was first proposed by Rydén and Lyngfelt [13]. Both in the mentioned work and in articles presented by other authors [11, 15, 16] the feasibility of the process based on thermodynamics has been displayed where the estimated efficiencies are competitive with conventional steam reforming without CO_2 capture. Spallina et al. [15] also estimated the hydrogen production cost for this option, which was competitive with conventional SMR with a low CO_2 avoidance cost. Other chemical-looping based alternatives for hydrogen production which are not based on externally heated reformer tubes are reviewed by Adánez et al. [14], Abad [17] and Luo et al. [18].

In order to achieve a H_2 production process with net negative CO_2 emissions it could be possible to use biomass instead of fossil fuel as supplementary fuel to the CLC system integrated with SMR [11]. Net negative emissions can be obtained since the carbon present in the biomass originates from CO_2 which has been withdrawn from the atmosphere through photosynthesis. Some new challenges are added, which are mainly connected to the risk of melting/slagging of biomass ash which could cause deposit formation on the reformer tubes if these tubes would be placed in the fuel reactor of the CLC system. In the referenced study [11] the reformer tubes were placed in an external fluidized bed heat exchanger but the air reactor could be another possible option. It should be mentioned that the biomass could potentially also be used as feed in the catalytic process in the reformer tubes with commercial steam reforming catalysts. However, this brings several additional challenges; for example, catalyst poisoning due to impurities such as sulphur, tar and alkali species [19, 20]. This option is not considered in this work.

Aims of the work

The aim of the thesis is to evaluate the potential to use fluidized bed heat exchangers as a heat source in steam reforming plants for hydrogen production. The thesis collects the main findings in four papers which all covers different aspects to assess the possibility of industrial implementation of the proposed processes. Additional details for each of these investigations can be found in the appended papers.

Paper I and **II** evaluates the thermodynamic performance of proposed processes where fluidized bed heat exchangers are integrated in steam reforming plants for hydrogen production. **Paper II** also presents an economic analysis of an industrial scale hydrogen production plant using a single fluidized bed heat exchanger with an oxygen carrier as bed material for in-bed fuel conversion. **Paper III** investigates oxygen carrier aided combustion, i.e. the possibility to increase the in-bed fuel conversion of methane, one of the key fuel components in the conventional steam reformer furnace, using oxygen carriers as bed material in a lab-scale BFB reactor. **Paper IV** investigates experimentally the bed-to-tube surface heat transfer at high bed temperatures for three different bed materials of various sizes and the determined heat transfer coefficients are compared with heat transfer correlations which could be used to predict the heat transfer to the steam reformer tubes in the targeted applications. Figure 2 illustrates the connection between the papers graphically.

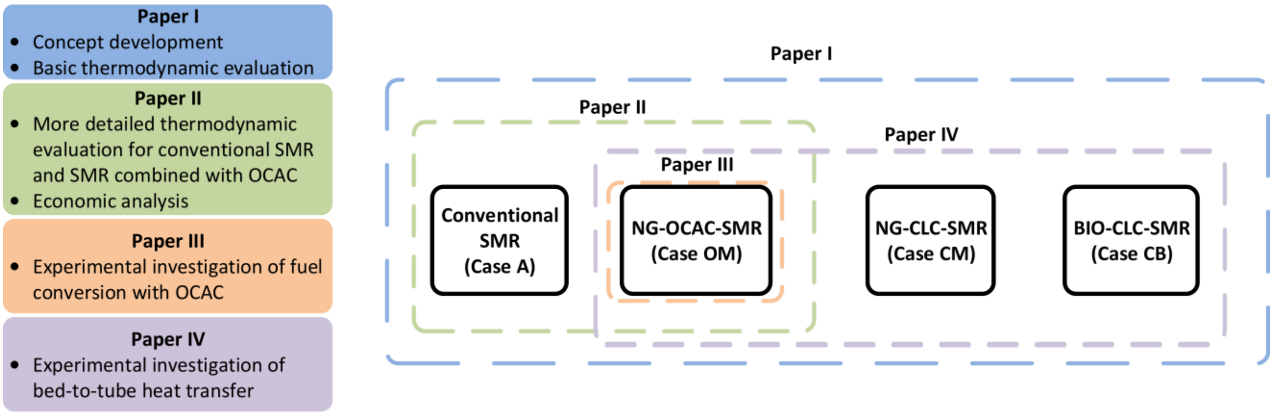
Paper I
Concept development
Basic thermodynamic evaluation
Paper II
More detailed thermodynamic evaluation for conventional SMR and SMR combined with OCAC
Economic analysis
Paper III
Experimental investigation of fuel conversion with OCAC
Paper IV
Experimental investigation of bed-to-tube heat transfer
Paper I
Paper II
Paper IV
Paper III
Conventional SMR (Case A)
NG-OCAC-SMR (Case OM)
NG-CLC-SMR (Case CM)
BIO-CLC-SMR (Case CB)

Figure 2. Illustration of the areas studied in the papers included in this thesis. SMR=Steam methane reforming, OCAC=Oxygen carrier aided combustion, CLC=Chemical-looping combustion, NG=Natural gas and BIO=Biomass.

Structure of the thesis

The thesis is organized as follows. This introduction is followed by Chapter 2 which provides a review of the literature describing conventional SMR technology as well as three key technologies related to the proposed processes. Chapter 3 presents the experimental setups consisting of reactors and materials used in the experiments in **Paper III** and **IV**. Chapter 4 presents the methodology used in the four papers where key assumptions in the presented models and the methods used in the experimental campaigns are described. Chapter 5 presents the main results and discusses the contribution of the individual results to the overall aim of this thesis. The main conclusions of this thesis are presented in Chapter 6 whereas suggestions for future studies are presented in Chapter 7.

2. Background

2.1. Steam Methane reforming

The conventional steam methane reforming (SMR) process is based on catalytic reforming of natural gas at high temperature, 800-950˚C and high pressure, 15-40 bar. The endothermic reaction, see Eq.(1), takes place in high-alloy reformer tubes where a catalyst, typically nickel-based [21], is placed on a pellets support material [22]. The tubes are heated by external gas burners hosted in a furnace where different tube and burner arrangements can be used [22].

$$CH_4 + H_2O \rightleftharpoons CO + 3\,H_2 \quad \Delta \mathrm{H}_0^{298\mathrm{K}} = 206.2\ \mathrm{kJ/mol} \tag{1}$$

The reformer is followed by one or more water-gas-shift (WGS) reactors to adjust the H_2/CO-ratio which in ammonia and hydrogen production plants should be as high as possible [22]. CO is converted according to the equilibrium-limited and slightly exothermic WGS reaction, see Eq.(2), which is favoured by low temperatures.

$$CO + H_2O \rightleftharpoons CO_2 + H_2 \quad \Delta \mathrm{H}_0^{298\mathrm{K}} = -41.2\ \mathrm{kJ/mol} \tag{2}$$

Product gas form the shift reactor is cooled to close to ambient temperature and further sent to a pressure swing absorber (PSA) where a high purity hydrogen stream is obtained, i.e., up to 99.999% purity [23]. A low pressure off-gas stream is generated which is rich in CO_2, but also combustible gases in form of CO, CH_4 and H_2. The off-gas is typically fed as fuel in the reformer furnace [23], together with supplementary fuel in form of natural gas. Combustion of off-gas and natural gas provides the heat for the endothermic reaction Eq.(1).

SMR plants typically generate significant amounts of excess heat, which in general should be avoided [22]. One of the main reasons for the excess heat generation is the limited heat transfer coefficients to the reformer tube surface, which constitutes the primary bottle neck for conversion of methane to synthesis gas. The driving force is mainly radiation, which requires combustion at very high temperatures in order to be sufficiently effective [24]. This results in flue gas with higher energy content than what can realistically be used internally within the process, i.e. excess heat production. The high temperatures which are required also results in thermal NO_x emissions. Therefore, since the heat transfer to the tube wall from the outside is typically the rate limiting step for reaction (1), the heat transfer to the tube wall could be improved and therefore a lower furnace temperature could be used which could: i) reduce the fuel consumption of supplementary fuel, ii) reduce the amount of excess heat generation, iii) reduce thermal NO_x emissions, iv) reduce the risk of temperature hotspots on the tube surface (a common reason for reformer tube failure) which is caused by uneven heat flux to the reformer tubes and is difficult to control by flame combustion.

2.2. Chemical-looping combustion

Chemical-looping combustion (CLC) is a process which can be used for heat and power production while providing inherent CO_2 capture. The CLC system, see Figure 3 consists of two reactor vessels, typically interconnected fluidized beds, and a solid oxygen carrier. In the air reactor the reduced oxygen carrier, Me_xO_{y-1}, is oxidized with air, Eq.(3). Me_xO_y is here a generic oxygen carrier. In the fuel reactor oxygen is released from the oxygen carrier by a gas-solid reaction with the fuel, Eq.(4).

$$(2j+k)Me_xO_{y-1} + (j+0.5k)O_2 \rightleftharpoons (2j+k)Me_xO_y \tag{3}$$

$$(2j+k)Me_xO_y + C_jH_{2k} \rightleftharpoons (2j+k)Me_xO_{y-1} + kH_2O + jCO_2 \tag{4}$$

By adding up Eq.(3) and (4), the total heat evolved in the system is found and this is equal to the heat released during normal combustion. Note that the oxygen is transported to the fuel reactor with the oxygen carrier, with the result that the flue gas stream from the fuel reactor is not diluted with N_2 and the CO_2 can be easily separated from the flue gas by steam condensation.

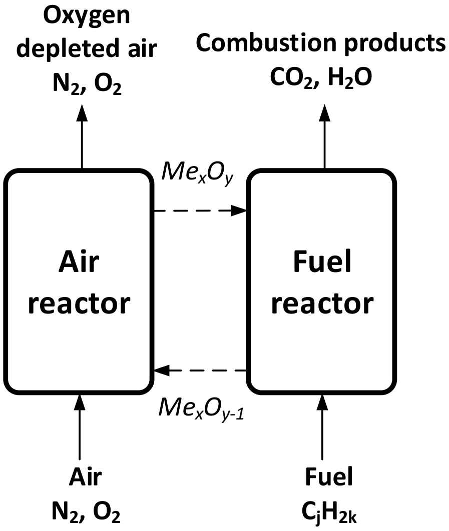

Figure 3. Schematic of chemical-looping combustion for a generic hydrocarbon fuel.

The energy balance of the two reactors depends on the oxygen carrier used, the temperature of the reactors and the fuel. While the oxidation of the oxygen carrier is always strongly exothermic the reduction of the oxygen carrier may be either endothermic or exothermic. Fe_2O_3 (hematite), NiO (nickel oxide), Mn_3O_4 (manganese oxide) and CuO (copper oxide) are commonly used as oxygen carriers [13]. The oxygen carriers can also be ores and minerals such as ilmenite, an iron-titanium oxide, waste materials containing metal oxides such as steel converter slag, also named LD slag, or manufactured oxygen carriers using different raw materials such as the calcium-manganese-based material $CaMn_{0.775}Mg_{0.1}Ti_{0.125}O_{3-\delta}$, also called C28. The technical requirements may differ depending on the application, but the oxygen carrier should in general have good fluidization properties, have a high reactivity and be resistant to mechanical stress. A summary of the current research status for CLC can be found in recent review articles [14, 25-27].

2.3. Oxygen carrier aided combustion

Oxygen carrier aided combustion (OCAC) is a combustion technology which has been recently proposed and tested [28]. The basic idea is to replace the inert bed material in fluidized bed boilers, typically silica sand in biomass boilers and waste incinerators with an oxygen carrier, similar to what is used in chemical-looping combustion (CLC). The presence of the oxygen carrier would introduce new fuel conversion mechanisms and the transport of oxygen in space and time [29, 30]. The oxygen carrier contains a metal-oxide which can undergo reduction and oxidation at the conditions in the fluidized bed combustion unit. The reactions are the same as presented in the previous section, Eq.(3) and (4).

The OCAC technology has been demonstrated in a 12 MW_{th} circulating fluidized bed boiler at Chalmers University of Technology which showed that the CO concentration in the flue gas leaving the boiler could be decreased by as much as 80% when using 40 wt.% ilmenite (a titanium-iron-ore), compared to operation with solely sand [28], while experiments with manganese ore and sand allowed for reduction with up to 70% for low air-fuel ratios [29]. Apart from minimizing emissions of carbon monoxide and unburnt hydrocarbons in conventional fluidized bed boilers, OCAC could also facilitate conversion of stable molecules such as methane in the dense zone of the fluidized bed. Because of the thermal inertia of the solids more stable fuel components, where methane is the most stable of all, do not easily burn in the dense bed, since the moderate temperature will effectively hinder ignition of the air-fuel mixture. This is not an issue in power plant since combustion will take place also in the freeboard above the dense bed, but if the goal is to provide heat directly to the fluidized bed solids for further transfer to the immersed tubes, this phenomenon could create problems. The fuel presented in the reformer furnace is a mix of mainly CH_4, CO and H_2 where CH_4 should be regarded as the most difficult fuel to oxidize.

However, CLC systems are examples of systems where complete conversion of methane/natural gas has been observed for several different oxygen carriers, i.e. under conditions without presence of air and at temperatures similar to the target temperature for this application [31-38]. It should also be mentioned that an oxygen carrier which is oxidized to a high extent is likely to have a higher reactivity. Provided that the amount of bed material is sufficient in relation to the fuel flow, OCAC should allow for direct conversion of methane in the dense fluidized bed. The effect of OCAC was observed in a study where the performance of sand and the oxygen carrier Fe_2O_3 was compared in a bubbling fluidized bed system for combustion of methane at 700°C. In this study it could be seen that essentially nothing happened inside the sand bed but as soon as only 0.13-1.3% of the bed mass was substituted with Fe_2O_3, methane was converted to a great extent within the bed [39]. Experimental campaigns with ilmenite [28], manganese ore [29] and steel converter slag [40] in a 12 MW_{th} CFB boiler with wood chips as fuel all indicated that partial substitution of the silica sand bed with these bed materials increased fuel conversion and therefore also the heat generation in the dense bed. This was indicated by the temperature at the top of the dense bed [29, 40] being higher when oxygen carrier was present in the bed compared to using only silica sand and the temperature drop in the cyclone [28, 29, 40] was more pronounced when oxygen carriers were present.

CO and H_2 which are the other fuel gases present in the reformer furnace, due to their presence in the PSA off-gas, are known to be more readily converted in fluidized bed reactors based on a higher reactivity with commonly used oxygen carriers [41, 42]. This motivates the focus on methane being the rate-limiting component. It should however also be noted that presence of CO and H_2 could support the conversion of methane in the targeted process.

In this thesis, one of the proposed processes involves implementation of OCAC in a single bubbling fluidized bed as a heat source for steam reforming where the steam reforming tubes are placed in the dense bed [11].

2.4. Fluidized bed heat exchanger

Fluidized beds are known to provide high heat transfer rates in the bed and almost uniform bed temperatures[43, 44]. As a result, there are many possible applications of using fluidized beds as heat sources in general. One such approach is to use so called fluidized bed heat exchangers (FBHEs), which consists of tubes immersed in the dense zone of bubbling fluidized beds. FBHEs are commonly placed after the cyclone in circulating fluidized bed (CFB) power plants, where the hot particles from the cyclone are cooled down in contact with the tubes (see Figure 4).

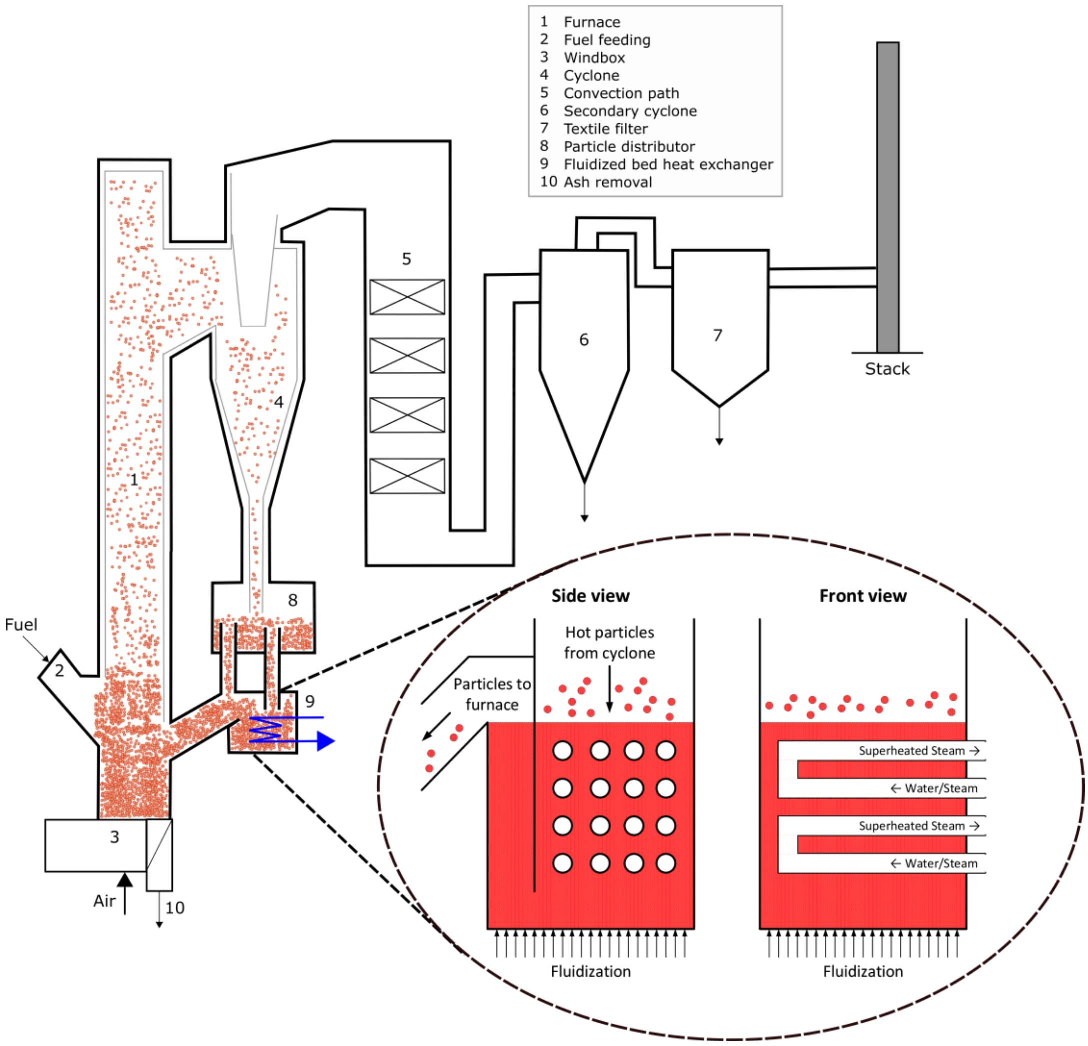
1 Furnace
2 Fuel feeding
3 Windbox
4 Cyclone
5 Convection path
6 Secondary cyclone
7 Textile filter
8 Particle distributor
9 Fluidized bed heat exchanger
10 Ash removal
Stack
Fuel
Air
Side view
Front view
Hot particles from cyclone
Particles to furnace
Superheated Steam →
← Water/Steam
Superheated Steam →
← Water/Steam
Fluidization
Fluidization

Figure 4. FBHE in circulating fluidized bed boiler.

The FBHEs are operated with a low superficial gas velocity, around 0.2-0.5 m/s to avoid tube erosion, with steam generation or superheating of steam taking place inside the tubes. These heat transfer surfaces improve the flexibility of the boiler significantly and can be used to control the superheat and reheat temperature, as well as the combustion temperature in the boiler. They can serve as an alternative to heat exchange surfaces inside the furnace or in the convection section [45].

Despite the favourable characteristics of fluidized bed heat exchangers, the use of FBHE at elevated temperature levels has so far been limited to water/steam-mixtures in immersed tubes for steam production. There are currently, to the best of the author's knowledge, no examples of implementations of FBHEs as a heat source for tubular chemical reactors. Using FBHEs as a heat source for steam reforming should be a most interesting possibility since it should be possible to achieve significantly improved conditions for heat transfer to the reformer tubes.

There are several models describing the heat transfer between a bed and a surface, one of them being the packet-renewal model [46]. According to this model, packets of particles are swept into contact with the heat transfer surface for a short period of time by the movements of bubbles. The first layer of particles in contact with the surface will cool down, or heat up if the surface is hotter than the bed. However, the packets are frequently replaced by new packets at bed temperature, resulting in a maintained high temperature difference between the bed particles and the surface. When theoretically determining the bed-to-tube heat transfer coefficient, convection from both gas and particles as well as radiation should be accounted for. It should however be mentioned that for small particle sizes (<1 mm) gas convection can generally be neglected [47].

Although FBHEs have been used in high temperature applications (i.e. >400˚C) there are few experimental studies to estimate the bed-to-tube heat transfer coefficient at high bed temperatures. Most of the research on heat transfer from bed to an immersed surface has recently been reviewed by Leckner et al. [44]. Despite much research done to determine correlations to provide predictive models for the bed-to-tube surface heat transfer, it is still difficult to make accurate predictive models in general [44]. In addition, some of the most well-known correlations to predict the heat transfer coefficient to a horizontal tube [47-52] are based on empirical correlations that have been determined at temperatures below 400°C, meaning that the correlations only include convective heat transfer. The bed-to-tube heat transfer coefficient which includes both convective and radiative heat transfer to the tube surface is therefore not so well-defined. It should also be mentioned that most of the previous work has been done with quite large bed particles which may not be the most suitable particle sizes for CFB/BFB/FBHE applications. Silica sand has been used in most these studies and to verify that the bed-to-tube heat transfer can be estimated also for other bed materials, additional experimental work is required.

3. Experimental setup

For the experiments presented in this thesis, two different reactors were used in the same furnace. The same infrastructure was used to feed gas to the reactor and measure temperature and pressure for both reactors. The two reactors are presented below where the differences in the setups are pointed out.

3.1. OCAC reactor

Experiments on OCAC is performed in a laboratory-scale high temperature steel reactor, see Figure 5. Air is fed as fluidization gas and a hole plate is used to provide a good gas distribution. Based on the risk of bed particles falling through the distribution plate a gas flow is always maintained through the windbox. The fuel gas flow, 99.5% methane, is introduced through a ring sparger located close to the distributor plate. The ring sparger is used to avoid the risk of fuel conversion already in the windbox and it is designed to distribute the fuel gas well over the entire cross section.

The hot gas leaving the BFB is fed to a ventilated hood which quickly cools it down. The reactor is placed in an electrically heated furnace with three heating zones which can be controlled separately, and where a target temperature can be specified for each zone. The temperature is measured in the windbox as well as at 8 vertical positions, MP1-MP8, both in the bed and in the freeboard, by means of thermocouples. The tubes where the thermocouples are introduced are also used to measure the pressure, by means of pressure transducers. At similar heights on the opposite side, corresponding to the same measurement point named MP1-MP8, gas can be extracted from the reactor. Gas sampling tubes with porous stainless steel metal filter plates welded to the ends are used to extract gas while preventing bed material from entering the gas sampling tube. Jacketed tubing is used on this side to make it possible to move the tube in the radial direction with teflon ferrules in the tube fittings.

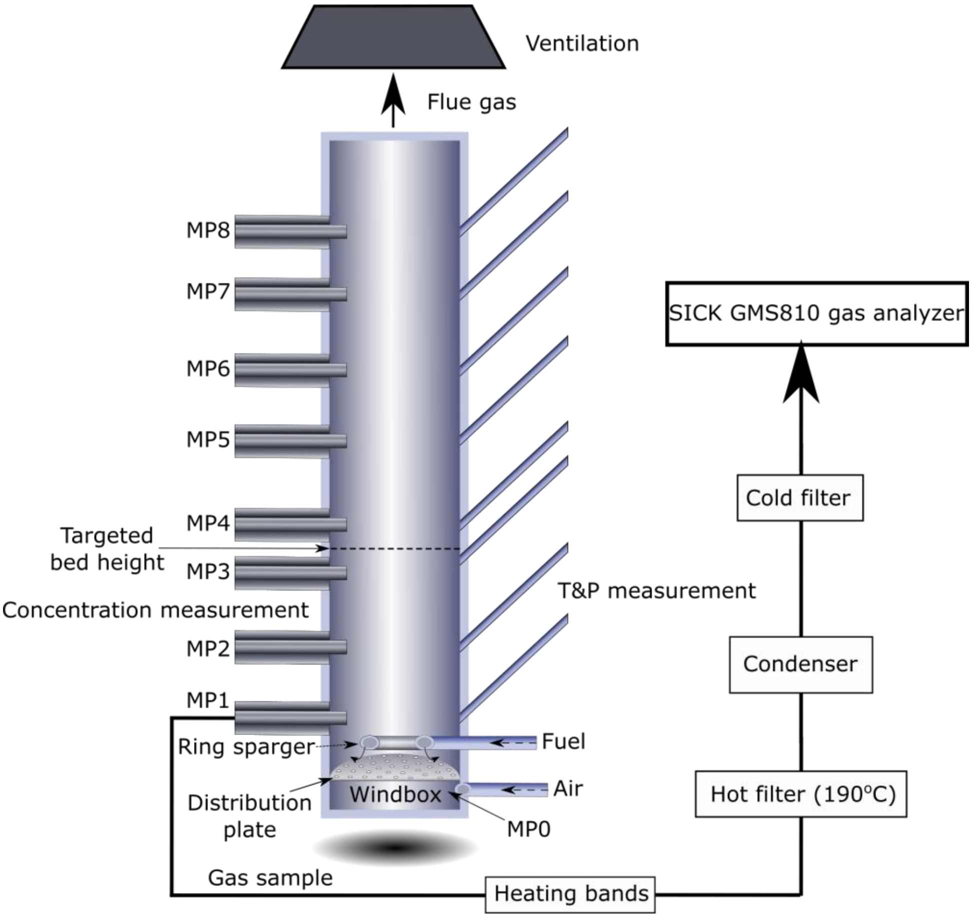
Ventilation
Flue gas
MP8
MP7
MP6
MP5
MP4
Targeted bed height
MP3
Concentration measurement
MP2
MP1
Ring sparger
Fuel
Distribution plate
Windbox
Air
MP0
Gas sample
Heating bands
T&P measurement
SICK GMS810 gas analyzer
Cold filter
Condenser
Hot filter (190°C)

Figure 5. Schematic illustration of the BFB reactor system with gas sampling tubes to the left and the inclined tubes for the pressure transducers and thermocouples to the right, each corresponding to a certain measurement point, MP1 to MP8.

During gas sampling, a heated line is attached to the measurement point of interest (MP1-MP8). The heated line is kept at a temperature of 190˚C to avoid condensation in the extracted gas stream. The sampled gases pass through a hot filter operating at the same temperature as the heated line. The wet gas is dried in a condenser followed by a cold filter before it enters to the gas analyser. Nondispersive infrared sensors, NDIR, are used to measure the concentration of CO, CO_2 and CH_4. O_2 is measured with a paramagnetic sensor and H_2 is detected using measurements based on thermal conductivity. All measurements are made online with one datapoint retrieved every second.

Equal volumes of bed materials were used in the experiments, meaning that the used bed mass was based on bulk density measurements prior to the experiments. The target was to have the bed height H_{bed}, defined as the top of the splash zone, between measurement points MP3 and MP4. Based on the measured gauge pressure at MP3, P_3, the bed height was therefore estimated according to Eq.(5). H_3 is the vertical position of MP3 above the distribution plate. The air density (ρ_g) is assumed to be negligible to the particle density (ρ_p) and the voidage of the fixed bed (ε_{fixed}) is assumed to be 0.4, whereas the voidage in the bubbling bed (ε_{BFB}) is assumed to be 0.6.

$$H_{bed} = H_3 + \frac{P_3}{9.81(\rho_p - \rho_g)(1 - \varepsilon_{BFB})} \tag{5}$$

The particle density was estimated based on the measured bulk density of the bed materials (ρ_b) according to Eq.(6).

$$\rho_p = \frac{\rho_b}{1 - \varepsilon_{fixed}} \tag{6}$$

The bulk density was estimated by measuring the mass poured into a known volume according to the ISO standard 3923-1:2008. The minimum fluidization velocity u_{mf} and the terminal velocity u_t presented in Table 1 are calculated for the particles fluidized in air at 700°C. The thermal input indicated in the same table is estimated for the case with a superficial gas velocity of 0.2 m/s, an air-fuel ratio of 1.05 and a temperature of 700°C.

Table 1. Bed material characteristics and bed inventory for the experiments in the OCAC reactor.

Position	Sand	Ilmenite
Mean particle diameter (µm)	136	149
Bulk density (kg/m^3)	1399	2204
Minimum fluidization velocity u_{mf} (m/s)	0.006	0.012
Terminal velocity u_t (m/s)	0.48	0.85
Solids inventory (g)	874.6	1378
Specific bed mass (kg/kW$_{th}$)	0.93	1.46

The two bed materials used in this investigation was Swedish silica sand from Baskarp supplied by Sibelco Nordic AB and Norwegian rock ilmenite supplied by Titania A/S. A size interval of 90-212 µm was chosen for both materials, where sieving was used to determine also the particle size distribution and the weighted mean particle diameter.

The sand is a practically inert bed material, with respect to oxygen carrying capacity, whereas the ilmenite is an oxygen carrier. The reaction between methane and the most oxidized state of ilmenite which is pseudobrookite (Fe_2TiO_5) and rutile (TiO_2) can be described according to Eq. (7).

$$\frac{1}{4}CH_4 + Fe_2TiO_5 + TiO_2 \Leftrightarrow 2FeTiO_3 + \frac{1}{4}CO_2 + \frac{1}{2}H_2O \quad \Delta H = 35\ kJ/mol\ O \tag{7}$$

The reoxidation of ilmenite can be described by Eq.(8).

$$2FeTiO_3 + \frac{1}{2}O_2 \Leftrightarrow Fe_2TiO_5 + TiO_2 \quad \Delta H = -235\ kJ/mol\ O \tag{8}$$

It should be noted that other reactions can occur as well, such as redox reactions with magnetite (Fe_3O_4) and hematite (Fe_2O_3).

3.2. FBHE reactor

The reactor used in the heat transfer experiments was of the same material and had the same overall dimensions as the OCAC reactor. The reactor is also operated as a bubbling fluidized bed, the main difference being a single horizontal tube made of Inconel alloy 600, with an outside diameter of 6 mm and the reactor can therefore be seen as a FBHE unit. The tube is placed 7.5 cm above the distribution plate which was welded to the outside wall of the reactor. The distribution plate was similar to the one presented for the OCAC reactor but with slightly smaller holes. Water is flowing inside the horizontal tube from a tap. The water flow rate is controlled with a valve and to measure the flow rate with high accuracy a scale is placed at the outlet. Pressure is measured at 5 different measurement points using pressure transducers. An outline of the reactor system can be seen in Figure 6.

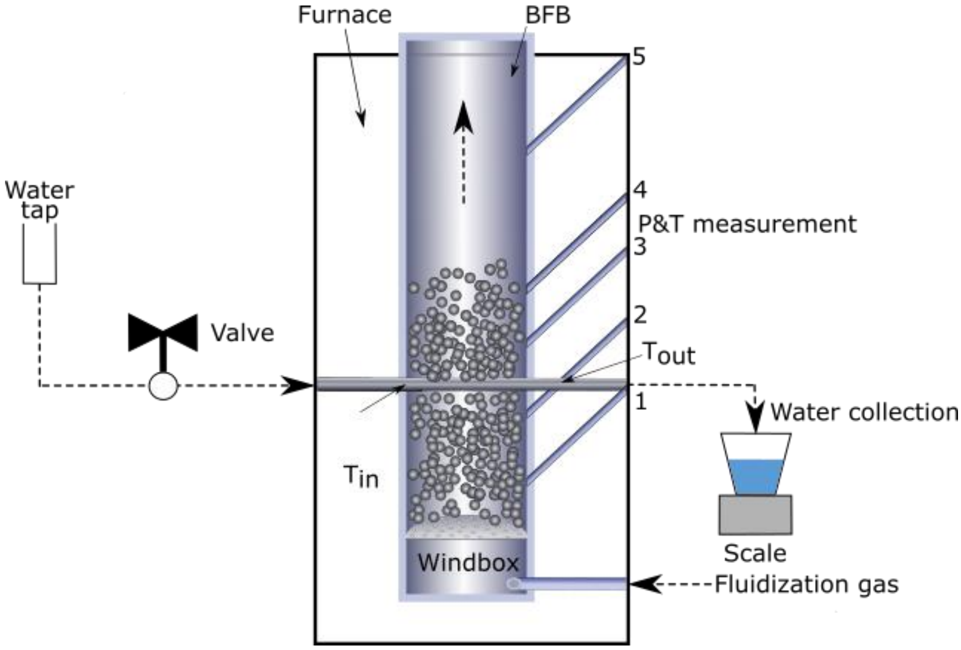

Figure 6. Schematic illustration of the BFB system with inclined tubes to the right for the pressure transducers and thermocouples indicating the different measurement points (1 to 5).

The temperature measured at measurement point 2 was defined to be used as the estimated bed temperature since it was considered to be at a suitable distance from the water tube to represent the temperature of the bed. The bed temperature is used in the calculations of superficial gas velocity as well as the heat transfer coefficient. Thermocouples were also installed at measurement point 1, 3 and 4. The temperature in the water tube was measured at the entrance point and the exit point of the BFB reactor, where the thermocouples were placed in the centre of the water tube.

The water tube at the outlet had to be bent around one of the inclined tubes to fit it inside the furnace, with the result that the thermocouple used to measure the outlet temperature of the water was placed approximately 2 cm from the inside BFB reactor wall. Based on an experiment in which the position at the water inlet to the BFB reactor was varied, it was concluded that this had negligible impact on the measured temperature at the outlet.

Thermocouples, type K, tolerance class 1, were used. The thermocouples were from the same batch, so the measured temperature should differ no more than 0.1°C between them. The thermocouples have a common reference point and are connected to a NI 9213 measurement module where the measurement is done in high-resolution mode with a measurement accuracy of <0.02°C.

Three different bed materials were used in this work. Equal volumes of bed material were used in all experiments, corresponding to a fixed bed height of 17 cm based on the measured bulk density. The bulk density was estimated using the same approach as for the OCAC reactor tests. The main characteristics of the fresh bed materials before adding them to the unit are presented in Table 2.

Table 2. Key characteristics of the bed material batches.

Bed material	Size range based on sieving [μm]	d_p [μm]	ρ_b [kg/m^3]	u_{mf} [m/s]	u_t [m/s]
Sand	90-212	129	1434	0.006	0.44
Ilmenite	90-212	167	2165	0.015	1.04
Ilmenite	250-355	280	2071	0.040	2.39
LD slag	90-150	123	1471	0.006	0.41
LD slag	150-300	199	1535	0.016	1.03
LD slag	300-355	327	1566	0.042	2.42

All materials were heat treated with air for at least 1 hour in the reactor system prior to the start of the experiments at 950˚C, to ensure that steady state properties of the bed materials were reached. Sibelco Nordic AB supplied silica sand from Baskarp, the most important sand source in Sweden. Silica sand is the most commonly used bed material in fluidized bed combustion of biomass and waste fuels and also the material which has been most frequently used in studies on heat transfer in fluidized beds. Titania A/S supplied the ilmenite which is physically beneficiated Norwegian rock ilmenite. Ilmenite is a mineral ore rich with titanium and iron oxides that is mined mainly for production of titanium dioxide. Ilmenite concentrate is a commonly used oxygen carrier in chemical-looping combustion systems for CO_2 capture, mainly due to its mechanical durability, non-toxicity and relatively low cost [27]. Ilmenite has also been successfully applied as bed material in fluidized bed boilers, where it has been shown to provide several benefits [53, 54]. Based on the possible use of ilmenite in fluidized bed processes it is considered interesting to also evaluate the heat transfer when using this bed material in relation to for example sand.

The material denoted as LD slag in this article is ground steel converter slag from the Linz-Donawitz production process. The material was provided by SSAB Merox AB. LD slag consists to a large extent of oxides of Ca, Mg, Fe, Si and Mn. Like ilmenite it is suitable as oxygen carrier in chemical-looping combustion [55, 56]. Large quantities of LD slag are generated but there is currently limited demand in many countries. Hence, due to good availability and potentially very low cost, the material could be suitable for large-scale operation in fluidized bed units, as has been shown recently [40]. Despite the indicated possible uses of ilmenite and LD slag, no previous studies on bed-to-tube heat transfer coefficient in a FBHE using these materials have been found which was an additional motivation. Both ilmenite and LD slag could be interesting bed materials in the processes presented in **Paper I** and **II**.

4. Methodology

The methodology applied in this thesis includes: 1) thermodynamic evaluation of three proposed processes where FBHEs are integrated in SMR plants in comparison with the conventional SMR process; 2) economic evaluation of one of these processes in comparison with conventional SMR; 3) experimental investigation of OCAC using methane as fuel with silica sand and ilmenite as bed materials; and 4) experimental investigation of bed-to-tube heat transfer to an immersed tube surface. The first two parts are to a great extent based on process simulation in Aspen Plus while the last two parts involves lab-scale experiments.

4.1. Thermodynamic evaluation of solutions with FBHE integrated with SMR for hydrogen production

The possibility to produce hydrogen by integration with OCAC and CLC (denoted by the letters O and C respectively) is evaluated in **Paper I**. A thermodynamic analysis is conducted to evaluate three alternative process configurations including fluidized bed heat exchangers in relation to a reference SMR plant with a gas-fired furnace as reformer furnace. Two of the proposed cases include the use of methane (M) as supplementary fuel while one of the CLC systems uses biomass (B). The three alternative process outlines are illustrated in Figure 7.

Case OM consists of a single fluidized bed heat exchanger which is used to heat the reformer tubes while case CM has the reformer tubes placed in the fuel reactor as part of a CLC system for CO_2 capture. The fuel reactor is operated as a BFB whereas the air reactor is operating as a CFB which provides circulation of the bed material. Case CB also includes a CLC system, but the reformer tubes are placed in an external FBHE which is interconnected with both air reactor (AR) and fuel reactor (FR). The external FBHE was proposed in **Paper I** based on the target to avoid interaction with potentially corrosive compounds in the biomass. The tubes were not placed in the AR in **Paper I** since it was assumed that this unit should be a CFB to provide circulation.

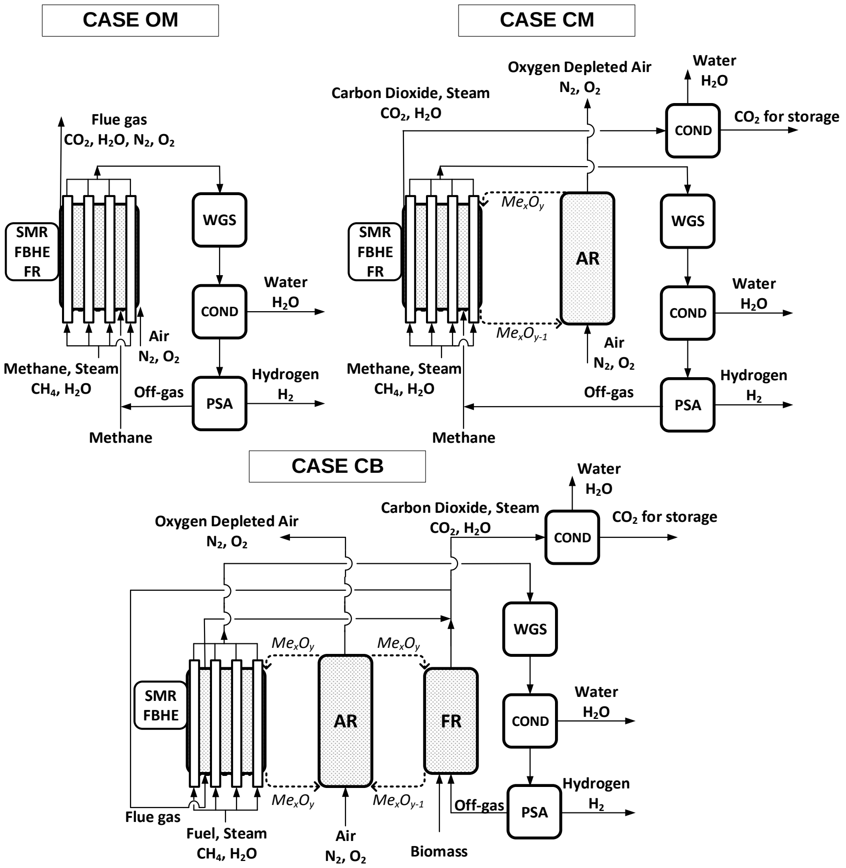
CASE OM
Flue gas
CO₂, H₂O, N₂, O₂
SMR
FBHE
FR
WGS
Water
H₂O
COND
Air
N₂, O₂
Methane, Steam
CH₄, H₂O
Off-gas
Hydrogen
H₂
PSA
Methane
CASE CM
Oxygen Depleted Air
N₂, O₂
Water
H₂O
Carbon Dioxide, Steam
CO₂, H₂O
COND
CO₂ for storage
MeₓOᵧ
SMR
FBHE
FR
AR
WGS
MeₓOᵧ₋₁
Air
N₂, O₂
COND
Water
H₂O
Methane, Steam
CH₄, H₂O
Off-gas
Hydrogen
H₂
PSA
Methane
CASE CB
Water
H₂O
Carbon Dioxide, Steam
CO₂, H₂O
Oxygen Depleted Air
N₂, O₂
COND
CO₂ for storage
WGS
MeₓOᵧ
MeₓOᵧ
SMR
FBHE
AR
FR
COND
Water
H₂O
Hydrogen
H₂
MeₓOᵧ
MeₓOᵧ₋₁
Off-gas
PSA
Flue gas
Fuel, Steam
CH₄, H₂O
Air
N₂, O₂
Biomass

Figure 7. Schematic illustration of the three alternative process configurations OM, CM and CB.

The purpose of the model used in **Paper I** was to identify and estimate the possible benefits of the different processes by estimating the hydrogen production efficiency (named cold gas efficiency in **Paper I**) which is based on the required fuel input per hydrogen produced. In addition to that, it was to estimate the decrease in waste heat generated in the alternative process configurations compared to the conventional process which is presented as case A.

In all studied cases in **Paper I** methane and steam at 25 bar is preheated to 650˚C before reaching the reformer. The produced syngas is leaving the reformer at 850˚C and cooled to 300˚C before it is fed to a low-temperature WGS reactor followed by another cooler to condense the steam. The steam is removed and thereafter the dry stream is fed to a PSA unit to separate the H_2 product stream with 100% purity. The off-gas stream from the PSA is fed to the reformer furnace, to which also supplementary fuel and preheated air at 600˚C is fed. The heat required for the steam reforming is withdrawn from the FBHE unit in case OM, CM and CB or from the gas-fired furnace (GFF) unit in case A. In the CLC-configurations, it is assumed that there is no temperature difference between the fluidized bed units. One of the key differences between case CB and the other cases in **Paper I** is that a higher hydrogen yield is achieved in the reformer which is motivated by the possibility to reduce the fossil input per hydrogen produced. This is done by using a higher steam-to-carbon ratio (5 instead of 3) and a higher outlet temperature from the reformer (900˚C instead of 850˚C).

In order to compare the four plant configurations, it was decided that all four plants should have the same external tube surface area. Several assumptions relating to the heat transfer in the conventional furnace and in the targeted fluidized bed heat exchangers are used to estimate the required flue gas temperatures in the respective processes. It should be accentuated that these estimations to compare the reformer furnace for the different cases in **Paper I** should be seen as rough estimations to visualize the potential of the proposed FBHE configuration. A better estimation can be done by presenting a possible FBHE design of suitable size and making more in depth calculations of the heat transfer in the reformer (see **Paper II**). For the pressure drop calculations the FBHE units were assumed to have a bed height of 5 m, bed voidage of 0.5 and a bed particle density of 2800 kg/m^3 and a distribution plate which provides a pressure drop corresponding to 30% of the pressure drop over the bed. This resulted in a pressure drop of 0.89 bar over the FBHE units. The pressure drop over the GFF in case A is neglected in this case. The other key assumptions for the four cases are presented in **Paper I**.

Models for the cases described in **Paper I** are included in an Aspen Plus simulation where a molar flowrate of 1 mol/s methane in the feed stream was used in all studied cases. The biomass supplied to case CB which is simulated as a typical gas composition of gasified biomass, has a Lower Heating Value (LHV) of 15 kJ/kg and consists of CH_4, CO, H_2 and C_3H_6 present in this combustible gas mixture. The air-fuel ratio for each case was calculated based on the known molar flows of the combustible products in the furnace. Additional assumptions included in the Aspen Plus model are presented in **Paper I**.

The thermodynamic evaluation presented in **Paper I** should be seen as a principal description of the concepts and identification of possible process configurations including both a single fluidized bed system and dual fluidized bed systems for CO_2 capture. In **Paper II** a much more complete flowsheet is provided for a reference SMR plant for hydrogen production (notified case A also in this paper) and the single FBHE system is presented as case OM also in **Paper II**. The flowsheet of case OM in **Paper II** can be observed in Figure 8.

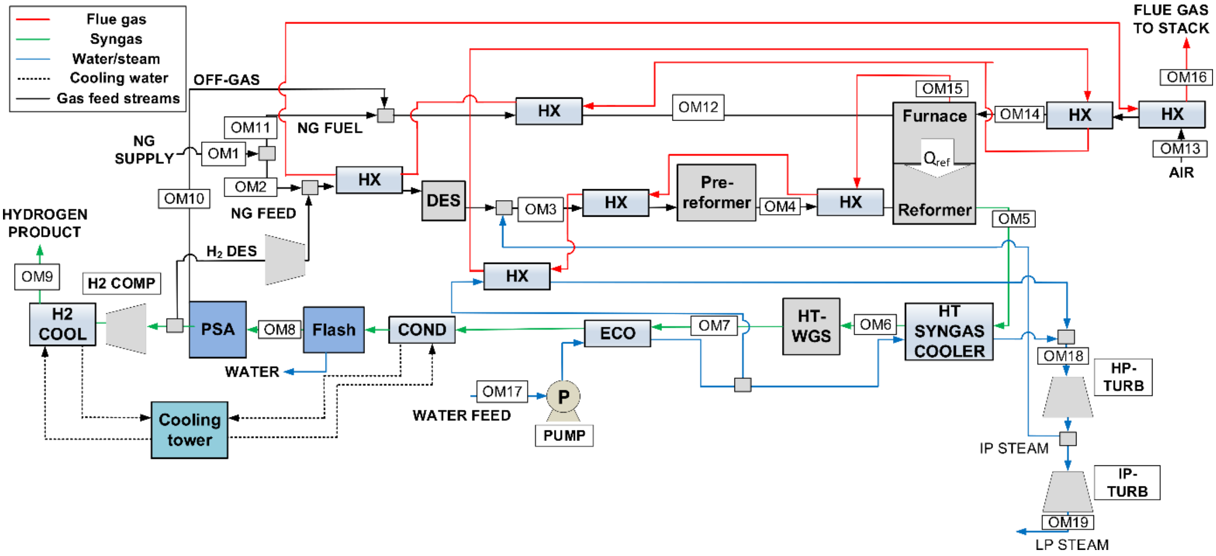
Flue gas
Syngas
Water/steam
Cooling water
Gas feed streams
OFF-GAS
NG FUEL
OM11
NG SUPPLY
OM1
OM2
OM10
NG FEED
HYDROGEN PRODUCT
H₂ DES
OM9
H2 COMP
H2 COOL
PSA
OM8
Flash
WATER
COND
Cooling tower
HX
DES
OM3
HX
HX
OM12
Pre-reformer
OM4
HX
OM15
Furnace
Q_ref
Reformer
OM14
HX
HX
FLUE GAS TO STACK
OM16
OM13
AIR
OM5
ECO
OM7
HT-WGS
OM6
HT SYNGAS COOLER
OM17
P
PUMP
WATER FEED
OM18
HP-TURB
IP STEAM
IP-TURB
OM19
LP STEAM

Figure 8: Schematic illustration of case OM where the reformer is integrated with a FBHE unit with OCAC. The scheme includes thermal integration with a steam cycle.

NG is used as supplementary fuel instead of using methane as in **Paper I**. The plant is also dimensioned to provide a target production rate of hydrogen suitable for a large-scale production plant. The plant also includes thermal integration with preheating of reactants and a heat recovery steam generator system, which produces intermediate pressure used in the steam reforming directly, as well as high pressure steam. A high pressure steam turbine and an intermediate pressure steam turbine are included in the model and the excess heat generation in form of low pressure steam is also evaluated. The model of the hydrogen production plant in **Paper II** also includes a more in-depth analysis of a possible FBHE design, choice of oxygen carrier and an evaluation of suitable operating parameters based on both hydrogen production efficiency and levelized hydrogen production cost.

Numerous possible performance indicators are possible for the two process plants compared in **Paper II**. The energy stored in the NG fed to the plant can be converted into hydrogen, electricity and heat. The possible use of electricity/heat can be related to the energy required to produce this electricity/heat in a state-of-the-art industrial plant. The approach presented by Martinez et al. [57] is used to compare the performance of the processes. The parameters used are summarized in Table 3 with Eq.(9)-(16).

Table 3. Parameters used in thermodynamic evaluation of the two plants.

Hydrogen production efficiency (%)	$\eta_{H_2} = \frac{\dot{m}_{H_2,prod} \cdot LHV_{H2}}{\dot{m}_{NG,tot} \cdot LHV_{NG}}$	(9)
Equivalent flow of CH_4 (mol/s)	$\dot{M}_{CH4,eq} = \dot{M}_{CH4} + \frac{7}{4}\dot{M}_{C2H6} + \frac{5}{2}\dot{M}_{C3H8} + \frac{13}{4}\dot{M}_{C4H10}$	(10)
Equivalent flow of NG (kg/s)	$\dot{m}_{NG,eq} = \dot{m}_{NG,tot} - \frac{Q_{th}}{\eta_{th,ref} \cdot LHV_{NG}} - \frac{W_{el}}{\eta_{el,ref} \cdot LHV_{NG}}$	(11)
Efficiencies reference plants	$\eta_{th,ref} = 0.9$ $\eta_{el,ref} = 0.583$	
Heat delivered from steam export	$Q_{th} = \dot{m}_{steam,exp} \cdot (h_{sat,vap,6bar} - h_{sat,liq,6bar})$	(12)
Hydrogen yield (%)	$Y_{H2} = \frac{\dot{M}_{H2}}{\dot{M}_{CH4,eq}}$	(13)
Equivalent hydrogen production efficiency (%)	$\eta_{H_2,eq} = \frac{\dot{m}_{H_2} \cdot LHV_{H_2}}{\dot{m}_{NG,eq} \cdot LHV_{NG}}$	(14)
Equivalent hydrogen production efficiency (based on that all LP steam converted to electricity in a LP steam turbine) (%)	$\eta'_{eq,H_2} = \frac{\dot{m}_{H_2} \cdot LHV_{H_2}}{\dot{m}_{NG,tot} \cdot LHV_{NG} - \frac{W'_{el}}{\eta_{el,ref}}}$	(15)
Conversion factor LP steam turbine	Electricity production LP steam turbine $= 0.1Q_{th}$	
CO_2 specific emissions ($g_{CO_2}/MJ_{H2\ produced}$)	$E_{CO_2} = \frac{\dot{m}_{CO_2,emitted}}{\dot{m}_{H2,prod} \cdot LHV_{H2}}$	(16)

W_{el} represents the net electricity production of the plant and W'_{el} is the sum of W_{el} and the electricity that could be produced by expanding the available LP steam in a LP steam turbine.

4.2. Economic evaluation of a single FBHE integrated with SMR for hydrogen production

The model of the hydrogen production plant in Aspen Plus is used as a basis for the economic assessment of the conventional SMR plant and the plant including a single FBHE integrated in a SMR plant. The economic analysis carried out in **Paper II** includes both capital and operational costs. A Bottom-Up Approach (BUA) is used where the cost of the most important components is estimated based the cost of reference components (C_o) with a similar function and the reference capacity S_o and scaled based on targeted capacity (S), see Eq.(17). The cost of the reference component is estimated for year x. The scale factor is represented as n and z is the number of required units of the reference component.

$$C = z \cdot C_o(\frac{S}{zS_o})^n \cdot \frac{CEPCI_{2015}}{CEPCI_{year\ x}} \tag{17}$$

The Chemical Engineering Plant Cost Index (CEPCI) is used to relate costs of process equipment for a certain year to the base year (2015). A Capital Charge Factor (CCF) is used to annualize the total cost to construct the operational plant and the fixed costs of the plant.

The equipment cost of the conventional gas-fired furnace (GFF) is estimated based on the cost estimation provided by Turton et al. [58]. The cost of a fluidized bed reactor is estimated based on cost estimation of a fuel reactor design provided by Bertsch within the EU-financed SUCCESS project [59] and the cost of the reformer tubes is added. The cost to replace the high alloy steel reformer tubes are based on the price indication provided by Roberts and Brightling [60] of 20000 US$/reformer tube. The reformer tubes in the conventional gas-fired furnace are assumed to have a life time of 50 000 hours in the conventional plant but twice as long in the FBHE, assuming the same tube material to be used.

4.3. Experimental investigation of OCAC in BFB

The OCAC experiments are carried out in the OCAC reactor described in chapter 3. The pressure and temperature were measured continuously for all measurement positions and the gas composition was measured continuously for one vertical position at a time. The targeted fuel flow was added to the system once the furnace had reached its setpoint value (600, 700 or 800°C) and measurement data was then extracted once steady state operation was observed with respect to measured pressure, temperature and gas concentrations.

When the gas sampling probe is placed at a certain height the gas concentration at that point is estimated as well as the average temperature and pressure at all measurement points. Average temperatures, pressures and gas concentrations were estimated at all measurement points apart from MP5 and MP8 where only temperature and pressure was measured.

The superficial gas velocity was kept at 0.2 m/s based on the set furnace temperature and the volumetric flow of air fed to the system. The experiments with varying air-fuel ratio (AFR) were operated with a fixed air flow and the fuel flow was decreased stepwise. The AFR is defined as the ratio of the volumetric flow rate of air fed to the fluidized bed to the volumetric flowrate corresponding to stoichiometric combustion of methane. The stoichiometric amount of air is based on the amount of oxygen needed to convert the methane fed to the reactor according to Eq.(18):

$$CH_4 + 2\,O_2 \rightarrow CO_2 + 2\,H_2O \qquad \Delta H_{298°C} = -802.3\ kJ/mol \tag{18}$$

The amount of unconverted methane (CH_4) can be related to the concentration of methane at the inlet since the reaction for combustion of methane is equimolar. If CO rather than CO_2 is detected it indicates that the combustion is incomplete, and the amount of detected CO can also be related to the inlet concentration of CH_4 since it is the only source of carbon fed to the system.

4.4. Experimental investigation of bed-to-tube surface heat transfer in FBHE

The average bed-to-tube surface heat transfer coefficient was experimentally determined by measuring the water temperature at the inlet and outlet from the reactor, as well as the water flow rate and the bed temperature. The heat transfer coefficient on the inside of the tube was determined using established correlations for liquid flow in tubes. The liquid was water with a temperature well below 100°C.

The gas flowrate fed to the fluidized bed was adjusted based on the bed temperature to obtain the targeted superficial gas velocity. One parameter at a time was adjusted, while keeping the others constant. The base case for the experiments was to operate with a bed temperature of 825˚C, a superficial gas velocity of 0.15 m/s and a water flowrate of 20 ml/s.

The heat load delivered to the water tube was estimated based on the temperature difference between inlet and outlet and the heat capacity of water. The overall heat transfer coefficient (U_o) could then be estimated based on the known tube surface area and the logarithmic mean temperature difference between the bed and the water. The temperature of the inside tube wall was estimated based on known heat load, inside heat transfer coefficient (see Eq.(19)) and the inside area of the tube.

$$T_{s,i} = \frac{Q}{h_i A_i} + T_{water} \tag{19}$$

The heat transfer coefficient through the wall and the temperature on the outside of the tube could then be estimated by using Eq.(20) and (21) through iterative calculations. The thermal conductivity of the tube wall is dependent on the wall temperature and it was estimated based on an average of the estimated temperature on the inside and outside tube surface.

$$h_w = \frac{2k_w}{d_o \ln{(d_o/d_i)}} \tag{20}$$

$$T_{s,o} = \frac{Q}{h_w A_o} + T_{s,i} \tag{21}$$

The estimated surface temperature on the outside of the water tube was also used to estimate the radiative heat transfer from bed to tube. The bed-to-tube heat transfer coefficient on the outside of the tube, h_o, including both radiative heat transfer and convective heat transfer was estimated using Eq.(22) [61].

$$h_o = \frac{1}{\frac{1}{U_o} - \frac{d_o \ln(d_o/d_i)}{2k_w} - \frac{d_o}{d_i h_i}} \tag{22}$$

The experimentally determined bed-to-tube surface heat transfer coefficient could also be compared with heat transfer correlations which can be used for prediction. These correlations have been determined using experiments performed by different researchers using a wide range of materials, equipment sizes and reactor configurations. Some of the most well-known correlations describing the bed-to-tube heat transfer coefficient were evaluated in **Paper IV** where these are presented in more depth [62].

All the heat transfer correlations presented have been established using a bed temperature below 400˚C and most of the correlations have used an electric heating rod to heat the fluidized bed which is opposite to principle of using the FBHE as a heat source as presented in **Paper I** and **II** for example. Based on the target of this study, which is to operate a BFB at high temperature, it is therefore important to verify if the presented heat transfer correlations could be used also for higher bed temperatures by comparing the experimentally determined heat transfer to the tube with the heat transfer predicted with heat transfer correlations.

In order to compare the estimated values for h_o, the radiative heat transfer coefficient was estimated (see Eq.(23)) where the emissivity of the bed, e_b, is estimated based on assumed particle emissivity ($e_b=0.5(1+e_p)$). The particle emissivity [61] and the emissivity of the tube wall surface [63], e_s, were both assumed to be assumed 0.9.

$$h_{rad} = \frac{\sigma\left((T_b + 273.15)^4 - (T_{s,o} + 273.15)^4\right)}{\left(\frac{1}{e_b} + \frac{1}{e_s} - 1\right)\left(T_b - T_{s,o}\right)} \tag{23}$$

Since the contribution from radiative and convective heat transfer to the tube surface are additive, the convective contribution was estimated as h_o - h_{rad}.

5. Results and discussion

5.1. Thermodynamic evaluation of solutions with FBHE integrated with SMR for hydrogen production

The key objective with **Paper I** was to evaluate basic thermodynamics of processes where FBHEs were used as a heat source for steam reforming. A parameter which was used to evaluate the thermodynamic performance of the plants was the hydrogen production efficiency (presented as cold gas efficiency in **Paper I**). This parameter is the ratio between the heat stored in the produced H_2 in relation to the total thermal input to the plant adding up the feed and supplementary fuel.

The first proposed process, named case OM, includes a single FBHE and it is the case which introduces the least new changes in relation to the reference plant. The use of the fluidized bed heat exchanger results in an improved heat transfer to the reformer tube enabling a lower flue gas temperature compared to the conventional reformer furnace. This lowers the supplementary fuel consumption and raises the hydrogen production efficiency from 76.4% to 79.4%, see Table 4. The reduction of the supplementary fuel consumption also leads to a reduction of the CO_2 emissions and the excess heat production is reduced mainly as a result of the reduced flue gas temperature from the reformer furnace.

Table 4. Specific process characteristics for all the studied cases.

Case	A	OM	CM	CB	
Hydrogen yield (%)	71.67	71.67	71.67	85.75	Ratio between hydrogen and the hydrogen which could be ideally produced from the hydrocarbons in the feed stream
T_{fg} (˚C)	1070	950	950	1000	Reformer furnace flue gas temperature
Supplementary fuel (%)	13.23	8.55	8.95	38.6	Additional fuel fed to the furnace in relation to the amount in feed (% on LHV basis)
η_{H_2} (%)	76.4	79.7	79.4	74.6	Hydrogen production efficiency based on LHV
CO_2 emissions (kg CO_2/m_n^3 H_2)	0.776	0.744	0	-0.391	Emissions of CO_2 for the overall process per m^3 produced H_2 at standard conditions
Change in CO_2 emissions (%)		-4.1	-100	-150.4	Change in CO_2 emissions in relation to the emissions for the conventional plant, case A
Excess heat (kW)	81.5	44.8	47.9	58.3	Excess heat above the pinch point
Thermal input (kW)	908.2	870.7	873.9	1111.5	Thermal input for the plant including feed and supplementary fuel
Share of thermal input (%)	9	5.15	5.5	5.24	Relation between excess heat to the thermal input

Case CM is similar to case OM, the main difference being that it has an additional fluidized bed reactor to enable inherent CO_2 capture using chemical-looping combustion. This addition increases the supplementary fuel consumption slightly and lowers the hydrogen production efficiency but with the added benefit of obtaining a process with net zero emissions of CO_2. The process is still significantly more efficient than the reference plant with a hydrogen production efficiency of 79.4%.

Case CB builds just as case CM on a CLC system, but the operational parameters are different as a result of the use of biomass as supplementary fuel. The target of this process is to obtain a system producing hydrogen while obtaining net negative emissions. To increase the amount of negative emissions, the supplementary fuel consumption of biomass can be increased in relation to the fossil input in the feed stream. By operating at a higher S/C ratio and a higher reformer outlet temperature it is possible to increase the hydrogen yield, i.e. the amount of hydrogen produced per hydrocarbon in the feed stream. The heat duty which must be transferred to the reformer tubes is higher in case CB compared to the other three processes which together with a higher targeted furnace temperature results in a higher supplementary fuel consumption. Although a higher hydrogen yield is reached in the process, the hydrogen production efficiency is reduced and the value is lower than for the conventional process, case A. The excess heat production is increased compared to case OM and CM but still clearly lower than for the conventional process when relating it to the total thermal input. The most interesting result from case CB is however that significant net negative emissions of CO_2 can be obtained from the process. Both case CM and CB could be highly attractive in a future energy system where significant emissions reductions are required.

All three proposed processes were considered interesting for a more detailed evaluation of the thermodynamics. **Paper II** presents a more detailed thermodynamic evaluation of two large-scale hydrogen production plants including one conventional SMR plant and a plant using a single FBHE.

A key design parameter in **Paper II** was the flue gas temperature in the reformer furnace in case A and OM and the estimation of this temperature was done using a much more elaborate approach than in **Paper I**. Based on the assumption that case A and case OM have equal reformer tube area, case OM allows for a significant reduction of the required flue gas temperature. The result of these calculations is visualized in Figure 9 and shown in Table 5 where the calculated heat transfer coefficients are presented as well as the logarithmic mean temperature difference for both cases. The temperature drop at the inlet of the reformer in Figure 9 is connected to the endothermic nature of the SMR reaction.

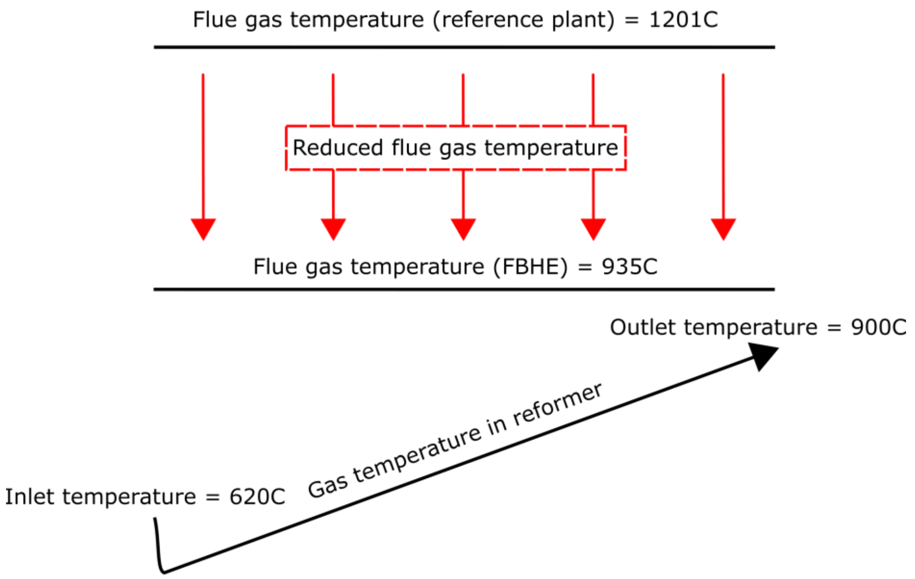
Flue gas temperature (reference plant) = 1201C
Reduced flue gas temperature
Flue gas temperature (FBHE) = 935C
Outlet temperature = 900C
Gas temperature in reformer
Inlet temperature = 620C

Figure 9. Illustration of the temperature profiles used in the model of case A and OM and the temperature of the gas in the reformer in **Paper II**.

The two plants presented in **Paper II** include more components and a more in-depth process configuration, more details of these plants are presented in **Paper II** but the most important results from the analysis are displayed in Table 5.

Table 5. Key results for the thermodynamic performance of case A and OM in Paper II.

		Case A	Case OM
Heat transfer coefficient inside reformer tube	W/(m^{2}K)	1384	1384
Heat transfer coefficient through tube wall	W/(m^{2}K)	2872	2872
Heat transfer coefficient outside reformer tube	W/(m^{2}K)	138	671
Overall heat transfer coefficient	W/(m^{2}K)	118	370
Logarithmic mean temperature difference	˚C	513	144
Reformer furnace flue gas temperature	˚C	1201	935
Net electric power	MW$_{el}$	12.3	2.6
Steam export (160˚C, 6 bar)	kg/s	18.8	4.1
Total NG consumption, $\dot{m}_{NG,tot}$	kg/s	9.10	8.15
H_2 production efficiency η_{H_2}	%	70.7	79.0
H_2 production efficiency $\eta_{H_{2,eq}}$	%	83.9	82.1
H_2 production efficiency η'_{eq,H_2}	%	75.8	80.2
CO_2 specific emissions, E_{CO_2}	$g_{CO_2}/MJ_{H2\ produced}$	80.7	72.2
Total CO_2 emissions	Mton CO_2/year	0.69	0.61

It can be observed that the flue gas temperature is significantly lower in case OM compared to case A and the estimated difference was larger than what was assumed in **Paper I**. The high flue gas temperature in case A is the main reason for excess heat production being significantly higher in case A in relation to case OM, where the assumed steam cycle delivers electricity and heat in excess in form of low-pressure steam at 6 bar. It can be observed in Table 5 that the excess electricity generation and the steam export is significantly higher for case A in relation to case OM. Excess heat generation is common for SMR plants and since the plant is assumed to be located at a refinery it is reasonable to assume that there is limited use of excess heat/electricity. The possibility to export excess electricity and the possibility to use this electricity for additional hydrogen production by electrolysis of water was evaluated as well but the possible economic benefits seem limited. Based on this assumption the hydrogen production efficiency $\eta_{\mathrm{H_2}}$, which only considers the produced hydrogen as a valuable output, is the most interesting parameter to consider. The hydrogen production efficiency is approximately 12% higher for case OM and the CO_2 emissions are reduced with a similar percentage. Case OM has thus advantages compared to the reference plant both from an economic point of view thanks to the possibility to reduce the fuel consumption and from an environmental point of view by reducing the CO_2 emissions from the process. The only situation where case A presents a higher hydrogen production efficiency is when both excess electricity and excess heat available as low-pressure steam, $\eta_{H_{2,eq}}$, can be utilized, which is not considered to be a reasonable scenario. The difference in the thermodynamic performance between case A and case OM was more pronounced in **Paper II** in relation to **Paper I**.

5.2. Economic evaluation of a single FBHE integrated with SMR for hydrogen production

Based on the thermodynamic performance of the three proposed processes case OM, CM and CB, the economics should also be evaluated for these systems. The economic assessment of case A and OM is presented in **Paper II**. The possibility to export electricity and heat was considered to have no economic value in this investigation. The key results of the economic assessment are presented in Table 6.

Table 6. Cost comparison between the two plants

Hydrogen production process		Case A	Case OM
Bare Erected Cost (M€ (% of total Bare Erected Cost, BEC))			
Desulfurization		0.71 (0.8%)	0.71 (0.8%)
HT WGS reactor		5.32 (5.9%)	5.32 (5.9%)
Reformer furnace		8.82 (9.7%)	10.88 (12.0%)
Pre-reformer		6.16 (6.8%)	6.16 (6.8%)
PSA unit		20.72 (22.9%)	20.72 (22.9%)
H_2 compressor		1.86 (2.1%)	1.86 (2.1%)
Air blower		-	0.28 (0.3%)
Steam turbine		7.79 (8.6%)	4.50 (5.0%)
Pump		0.24 (0.3%)	0.20 (0.2%)
Syngas cooling HX		10.57 (11.7%)	13.05 (14.4%)
Flue gas cooling HX		24.95 (27.5%)	21.78 (24.0%)
Cooling water system		3.44 (3.8%)	5.10 (5.6%)
Bare Erected Cost (BEC)	M€	90.6	90.6
Total Plant Cost (TPC)	M€	213.8	213.7
Total Plant Cost	M€/year	30.9	30.9
O&M fixed costs (M€ (% of total O&M fixed costs))			
Labour costs		1.20 (7.9%)	1.20 (8.7%)
Maintenance cost		5.34 (35.2%)	5.34 (38.7%)
Insurance cost		4.28 (28.2%)	4.28 (31.0%)
WGS catalyst		0.19 (1.2%)	0.19 (1.3%)
Reformer tube replacement		1.22 (8.0%)	0.61 (4.4%)
Pre-reformer and reformer catalyst		1.31 (8.6%)	1.31 (9.5%)
Desulfurization catalyst		0.33 (2.2%)	0.33 (2.3%)
Internal + external insulation		1.33 (8.8%)	0.56 (4.1%)
Total O&M fixed costs	M€/year	15.2	13.8
O&M variable costs (M€ (% of total O&M variable costs))			
Cooling water make-up		0.06 (0%)	0.10 (0.1%)
Process water		0.71 (0.5%)	0.71 (0.5%)
Oxygen carrier make-up		-	2.1 (1.6%)
Natural gas		140.2 (99.5%)	125.6 (97.7%)
Total O&M variable cost	M€/year	140.9	128.5
Hydrogen production cost (including all the above costs)			
LCOH	$€/Nm^3_{H_2}$	0.237	0.220
LCOH	$€/kg_{H_2}$	2.639	2.443

It can be observed in Table 6 that the estimated total equipment costs for the two systems are similar. The reformer furnace is larger in case OM mainly as a result of the limitation in the gas velocity in the FBHE which results in a higher cost of this unit compared to the reference plant. The difference in unit cost is however small since the reformer tubes are estimated to make up a major share of the cost of the reformer. The steam turbines and the heat exchange surfaces are more expensive in case A in relation to case OM. The O&M fixed costs are similar for the two cases. The main reason for the difference in the levelized hydrogen production cost between case A and OM is the cost of the fuel which is 14.6 M€/year lower for case OM as a result of a higher production efficiency. The Levelized Cost of Hydrogen, LCOH, is more than 7% lower for case OM than for the conventional

SMR production plant which indicates that this technology could be very interesting for large-scale hydrogen production. It is conceivable that case OM could also serve as a first step towards the integration of a chemical-looping combustion system allowing for inherent CO_2 capture (case CM) at a limited added cost.

In the sensitivity analysis, it was observed that the cost to replace the oxygen carrier in the process is not negligible and cheaper bed materials could be of interest. Furthermore, it is important to maintain a high availability of the plant to compete with the conventional SMR. Since almost all components are identical in the two plants, the difference in availability should depend on the operability of the reformer furnace which is difficult to assess at this stage without long term testing at a suitable scale.

5.3. Experimental investigation of OCAC in BFB

The component in the fuel gas which is considered to be the most difficult to burn is methane. The main aim of **Paper III** was to investigate if methane could be converted in the bed at moderate temperatures and to study the influence of the bed material by a comparison of silica sand and an oxygen carrier. Figure 10 presents the vertical concentration profile of methane in relation to the methane fed through the ring sparger at different furnace temperatures.

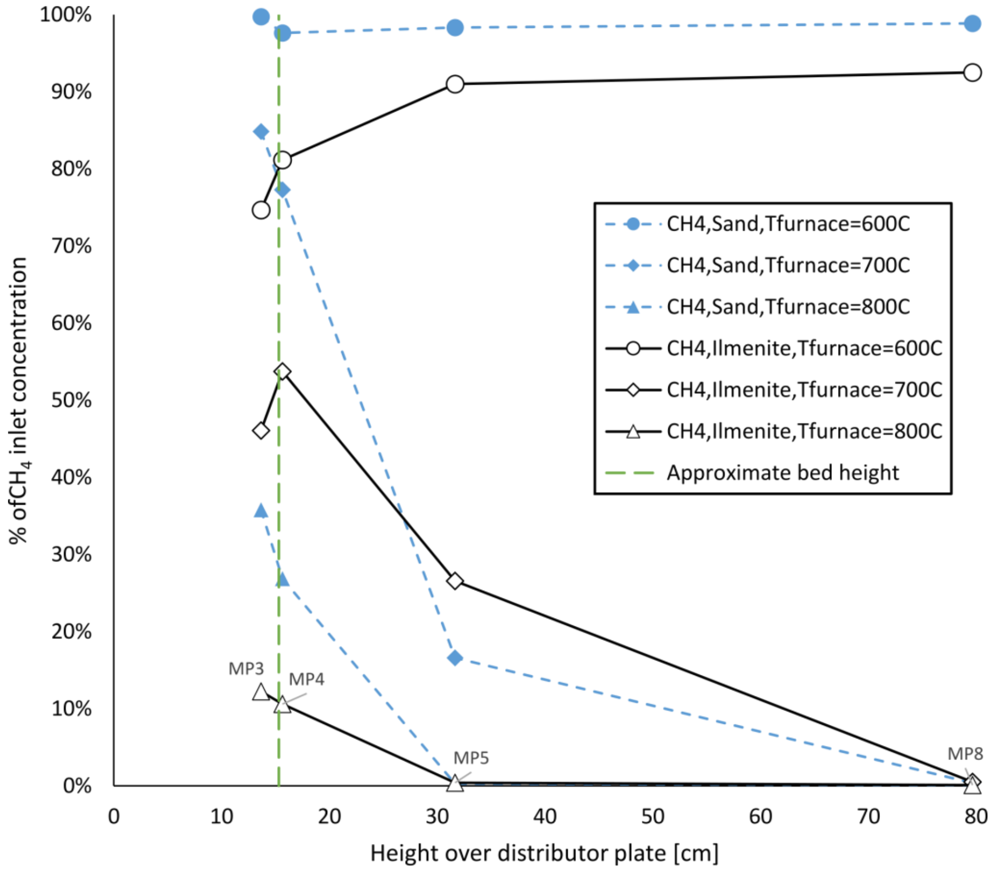

Figure 10. Measured gas concentration of CH_4 at different distances from the distributor plate (MP3, MP4, MP5 and MP8) at the furnace temperatures (600, 700 and 800˚C) for sand and ilmenite.

It can be observed in Figure 10 that increasing furnace temperature results in a higher conversion of methane as expected. At the highest furnace temperature most of the methane is already burnt at MP4. When comparing ilmenite and sand it can be observed that the concentration of methane is lower in the bed with ilmenite at all three furnace setpoints. This shows that the use of an oxygen carrier such as ilmenite increases the in-bed fuel conversion compared to using an inert bed material such as sand, which is a key result of this experimental campaign. When comparing the temperature in the bed in the two systems, see Figure 11, it could be observed that the bed temperature was slightly higher in the ilmenite system and the difference was larger at lower furnace setpoint temperatures.

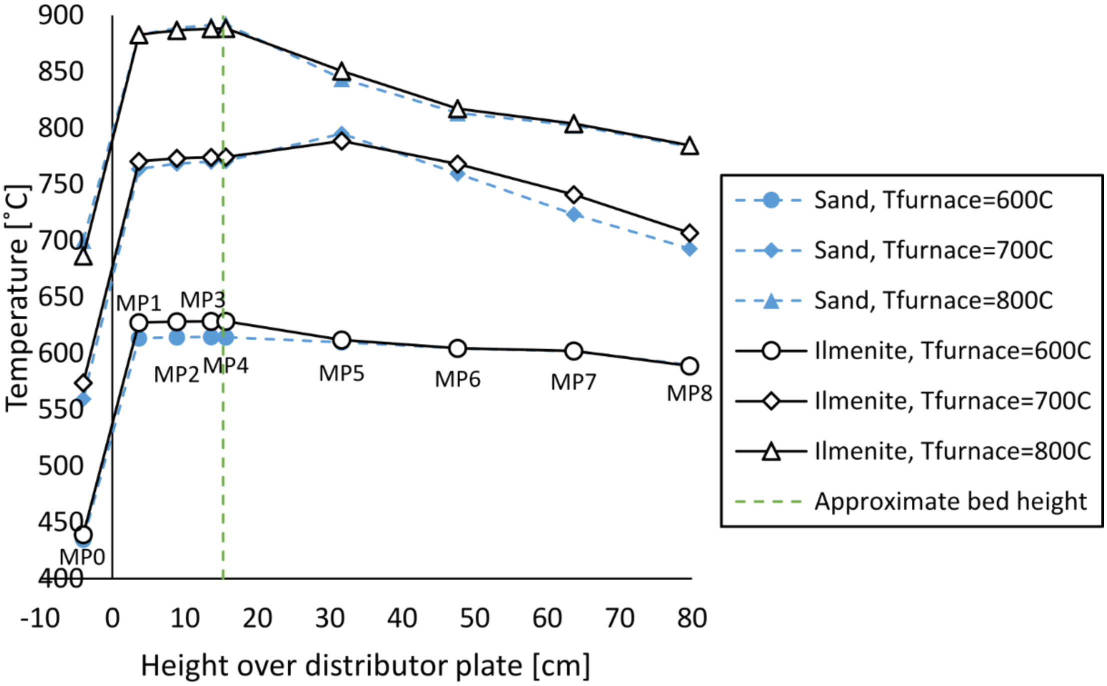

Figure 11. Measured temperatures at different distances from the distributor plate at three different furnace temperatures (600, 700 and 800˚C) for both sand and ilmenite.

This indicates that the use of oxygen carriers can increase the in-bed fuel conversion of methane and the heat generation in the dense bed. With respect to ilmenite it should be mentioned that the reaction between methane and ilmenite itself is endothermic but the reoxidation is exothermic and the net heat release corresponds to the heat of combustion for methane. It can be noted that the CH_4 concentration is higher with ilmenite at MP5 at 700˚C furnace temperature. This is likely an artefact caused by that the ilmenite was not sufficiently oxidized at this moderate bed temperature leading to the there was a net adsorption of oxygen to the bed during the experiments. This led to that the oxygen concentration in the freeboard was lower than it should be with ilmenite during steady state-operation. It should have been possible to reach a steady state process if the bed had been heat treated in an oxidizing atmosphere at a higher temperature which should be done in the future experiments. The material properties of ilmenite are known to change during the first redox cycles and it would have been better to operate the material for numerous hours to reach its steady-state properties before the start of the experiments. One of the characteristics known to improve after longer operation is the reactivity with fuel gases, and it is therefore likely that the in-bed fuel conversion would have been even higher with heat treatment at higher temperature prior to the experiments instead of using fresh particles.

When studying a varied air-fuel ratio between 1 and 1.2 at a superficial gas velocity of 0.2 m/s and a furnace setpoint temperature of 700˚C it was observed that the methane concentration was consistently lower with ilmenite as bed material for all air-fuel ratios. In order to increase the in-bed fuel conversion at these moderate temperatures it is clear that substitution of inert bed material with oxygen carrier is more effective than increasing the AFR-ratio.

The results of **Paper III** are useful when considering the fluidized bed processes proposed in **Paper I** and **II**, in particular the system based on OCAC. The experiments show that it is possible to convert CH_4 in the bed which is important to achieve also in the proposed processes presented in **Paper I** and **II.** It should however be mentioned that there are several differences between the experimental unit and the FBHE unit proposed for OCAC. First of all, the scale of the unit is much smaller than the proposed industrial scale unit. Operation with a deep bed could increase the risk of poor gas-solids contact in general due to bubble growth. Bubble size could however be reduced by use of internals in form of small horizontal tubes or packing material. Secondly, the temperature in the proposed FBHE is higher which is expected to provide even higher fuel conversion in the bed. Thirdly, the fuel gas in the targeted application include in addition to CH_4, also H_2 and CO as the main burnable fuel components and based on CH_4 being the most difficult fuel to convert in the fuel gas, it should be expected that higher fuel conversion rates can be achieved in the targeted application. This has been shown experimentally in lab-scale tests with Fe-based oxygen carriers where the combustion efficiency was higher for PSA off-gas compared to CH_4 [42]. Fourthly, it should also be mentioned that there are many oxygen carriers which have a higher reactivity towards methane than ilmenite, such as C28 which was mentioned previously. If a more reactive oxygen carrier would be used it should be possible to obtain an even higher dense bed fuel conversion. The assumptions used in **Paper I** and **II**, that a high fuel conversion can be expected to enable a transfer of the heat of combustion to the reformer tubes, are reasonable based on the experimental results in **Paper III**.

5.4. Experimental investigation of bed-to-tube surface heat transfer in FBHE

The key reason for the improvement in hydrogen production efficiency and a lower LCOH for case OM in relation to case A presented in **Paper I** and **II** is the improvement in heat transfer to the reformer tubes. This was investigated further in **Paper IV** and the results from the experimental investigation in a FBHE reactor using six different material batches for three different bed materials is presented in this section. One of the main targets of the experimental study on the bed-to-tube surface heat transfer coefficient in a FBHE was to verify that high heat transfer coefficients can be expected in a bed at high bed temperatures which is targeted for the proposed processes. The key experiment to verify this was conducted by varying the bed temperature between 400-950˚C using a superficial gas velocity of 0.15 m/s for all bed material batches. The result can be observed in Figure 12. High bed-to-tube surface heat transfer coefficients, 768-1858 W/(m^2K), were observed where the heat transfer coefficient seemed to increase almost linearly with bed temperature.

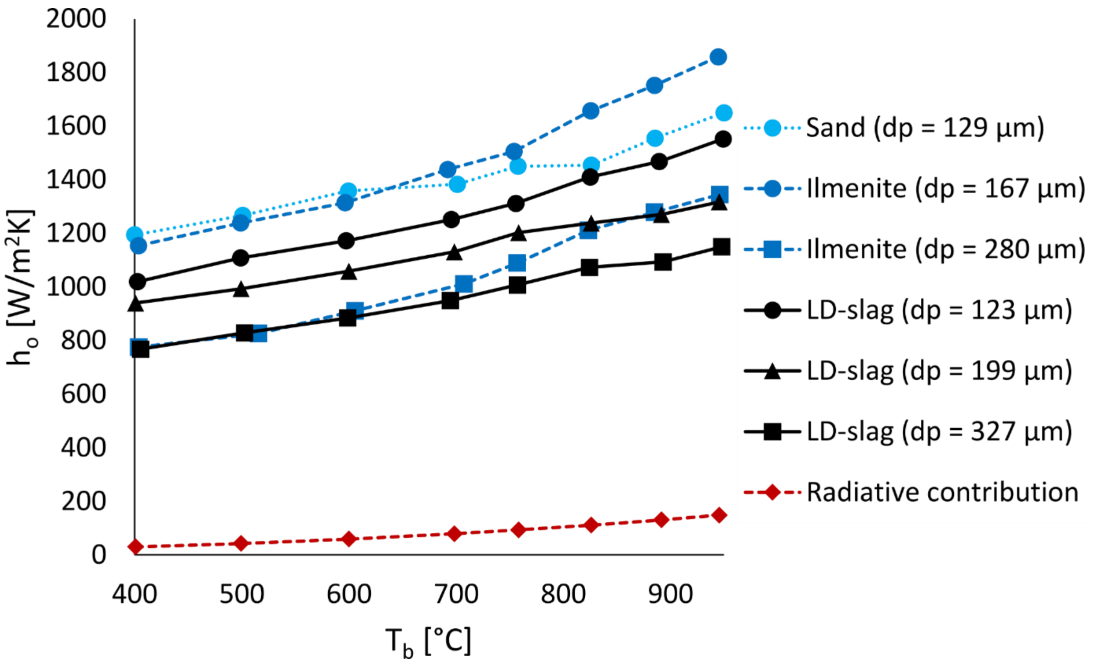

Figure 12. Estimated heat transfer coefficient at different bed temperatures.

The effect of increasing bed temperature on bed-to-tube heat transfer is expected since the heat transfer from both radiation and convection is expected to increase with increasing bed temperature. A general trend which can be observed is that the heat transfer coefficient increases with decreasing particle size. This is also expected since smaller particles are in general more efficient in exchanging heat with the tube surface. Another observation which can be made is that the radiative heat transfer contribution to the overall heat transfer to the tube appears to be small although the estimated radiative heat transfer coefficient is increasing with increasing bed temperature. The estimated radiative heat transfer h_{rad} was very similar for all bed materials where the estimated temperature on the outside of the tube was the only difference. This motivated the use of a single line in the figure indicating the radiative heat transfer coefficient h_{rad}. The contribution from radiative heat transfer in relation to the convective heat transfer increased slightly with particle size.

The estimated heat transfer coefficients in this paper was also compared with other studies at high bed temperature to determine if it is reasonable to expect the high values as the ones found in this study. Andersson presents a review of such studies with a single tube FBHE units at high temperature where particle diameters of 465-584 µm were used and the estimated values were in the range 400-700 W/(m^{2}K) [64]. This indicates that the absolute values estimated in this work for the bed-to-tube heat transfer coefficient are reasonable since a significantly smaller particle size is used in the experiments in **Paper IV**.

When considering the possible application of using a fluidized bed as a heat source for endothermic processes such as steam reforming, as presented in **Paper I** and **II**, it is important to have an adequate prediction of the bed-to-tube heat transfer coefficient. The experimentally determined heat transfer coefficients were therefore compared with heat transfer correlations. Most of the experimental research on bed-to-tube heat transfer has been done using bed temperatures below 400˚C. Since some of the most well-known heat transfer correlations have been determined at these low bed temperatures and it may be questioned if these correlations could be applicable also for higher bed temperatures. The second target of **Paper IV** was therefore to evaluate if these heat transfer correlations can be applied to high bed temperature applications such as the processes based on fluidized bed heat exchangers presented in **Paper I** and **II**.

Heat transfer correlations were used to predict the bed-to-tube surface heat transfer coefficient for all six material batches. These values were compared with the experimentally determined values where the result of this comparison can be observed in Figure 13.

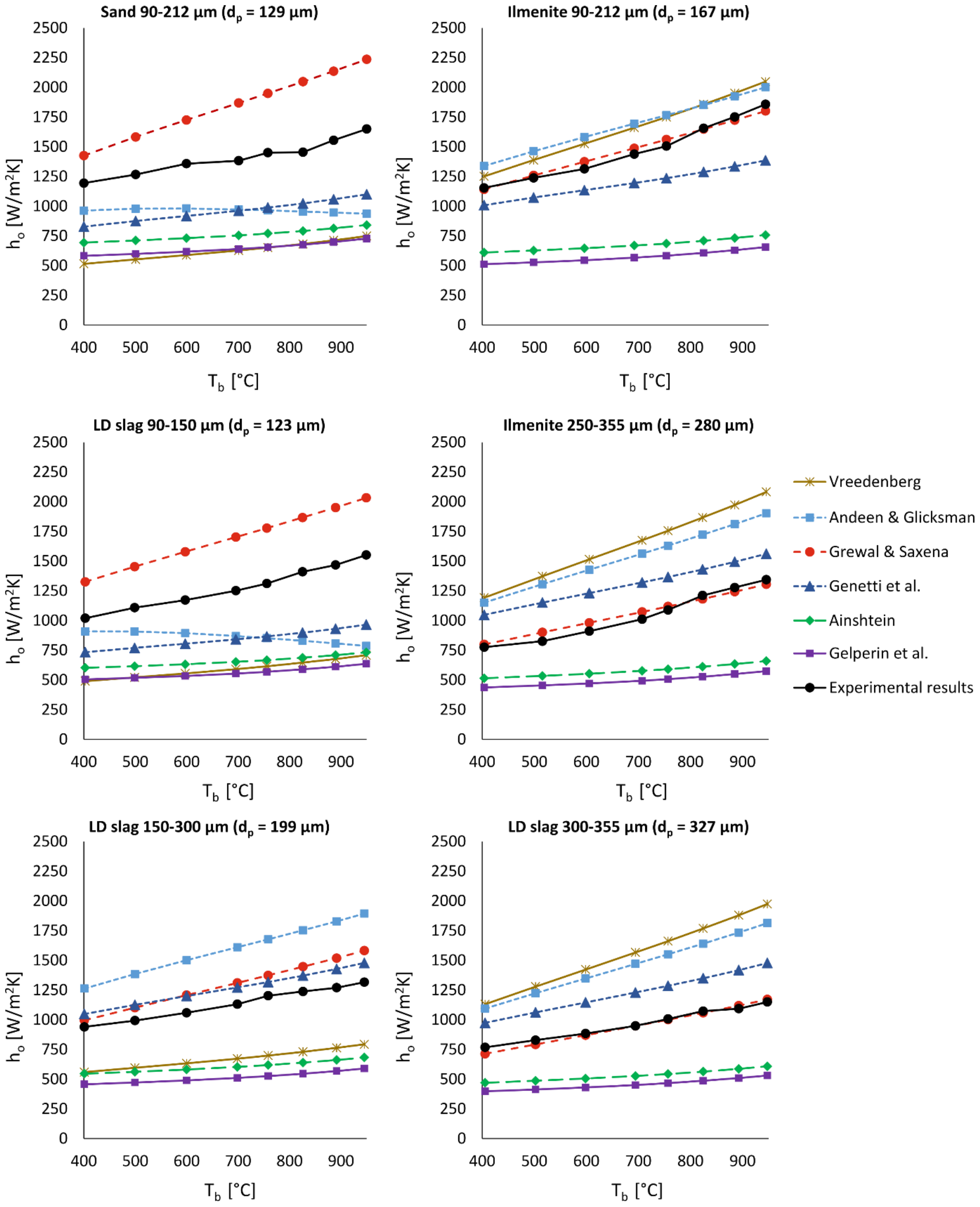

Figure 13. Comparison of the experimental data with the studied correlations for each tested material batch.

It can be observed that there is a significant spread between the heat transfer correlations. It is well-known that it is difficult to predict the heat transfer coefficient for a varied range of experimental conditions [47] as for example a range of gas velocities. It should also be mentioned that the correlations are semi-empirical and determined at low or moderate bed temperatures and it is not obvious that these expressions can be extrapolated to determine the heat transfer coefficient also at high bed temperatures. It is therefore expected that these heat transfer correlations have difficulties to accurately estimate the heat transfer coefficient for these six material batches.

All included heat transfer correlations have difficulties to predict the heat transfer coefficient accurately for the two material batches with the smallest mean particle size. For the other four material batches it is however clear that Grewal & Saxena manages to predict with a very high accuracy. This correlation also seems to predict the trend with increasing bed temperature at a satisfactory level.

The heat transfer correlations of Grewal & Saxena and Genetti are considered to predict the bed-to-tube surface heat transfer coefficient with a high accuracy since these correlations have a Root-mean-square (RMS) error of less than 30% compared to the experimentally determined h_o. In this comparison only the convective heat transfer contribution was included so the radiative contribution was removed from both of the estimated values. The RMS error for Andeen & Glicksman was within 40% which is considered accurate. The other correlations are considered to be not so accurate at predicting the bed-to-tube heat transfer coefficient in this unit.

Although some of the correlations are not so accurate at predicting the convective heat transfer coefficients, the absolute values for the heat transfer coefficients estimated in **Paper IV** are in the expected range. Based on this experimental investigation it seems possible to use heat transfer correlations to predict the bed-to-tube heat transfer coefficient also for high temperature applications such as the FBHE designs for heat extraction to SMR. The assumptions used for the bed-to-tube heat transfer in the models presented in **Paper I** and **II** seem to be reasonable or even rather conservative based on the results observed in **Paper IV**. As pointed out in earlier sections the idea is to use vertical tube bundles in the steam reforming application whereas a single horizontal tube is used in the experimental setup. Another difference is that the gas used in the steam reforming furnace is a flue gas with high CO_2 content whereas the fluidization gas in the experimental setup is air. All the mentioned differences are however considered in **Paper II** when using heat transfer correlations to estimate the bed-to-tube surface heat transfer coefficient.

It should be mentioned that even though high heat transfer coefficients are observed for all bed materials tested, there are significant differences between the three tested bed materials, especially when comparing ilmenite and the other two tested bed materials. This is, at this point, not so well understood, mainly due to lack of data concerning the material properties. Although differences may be observed between different bed materials, high heat transfer coefficients should be expected for any bed material and the benefits from using FBHEs as a heat source for steam reforming instead of using a gas-fired furnace are considerable. Based on the high heat transfer coefficients which can be expected in FBHEs, several alternate FBHE design solutions are possible and still obtain significant benefits compared to the conventional process mainly in terms of allowing for a reduction in the required flue gas temperature from the reformer furnace as presented in **Paper I** and **II** through a more efficient heat exchange to the reformer tubes.

6. Conclusions

All three proposed processes using integration of fluidized bed heat exchangers in SMR plants for hydrogen production show higher performance when compared with a conventional SMR plant. The main difference is the possibility to provide a more efficient heat transfer to the reformer tubes in the fluidized bed which opens up possibilities for reducing fuel consumption, excess heat generation and CO_2 emissions. Two of these suggested systems are integrated with chemical-looping combustion which include the possibility of CO_2 capture and one of these cases is using biomass as supplementary fuel thus presenting an opportunity for net negative CO_2 emissions.

The techno-economic evaluation of a targeted large-scale hydrogen production plant displays that the option to use a single fluidized bed heat exchanger as a heat source for steam reforming presents a 12% higher hydrogen production efficiency and a 7% lower levelized hydrogen production cost compared to the conventional SMR process. This shows that the process should be of interest for industrial implementation.

An experimental investigation of OCAC at moderate temperatures with methane supports the hypothesis that efficient in-bed fuel conversion of the fuel gases can be achieved using oxygen carriers as bed material.

An experimental investigation using a high temperature FBHE reactor supports the hypothesis that high heat transfer coefficients can be achieved from bed to tube surface and that well-known heat transfer correlations can be used to estimate the heat transfer coefficient from bed to tube for the proposed application.

7. Future work

During the experimental campaign with OCAC the heat treatment of the oxygen carrier ilmenite was not satisfactory. For the next campaign heat treatment should be conducted at a higher temperature in presence of oxygen to ensure that there is no net adsorption of oxygen during the experiment, as was the case with ilmenite at low bed temperature. The injection of the fuel into the bed may also be improved to secure a good fuel distribution in the bed without having the risk of combustion of the fuel in the windbox. Other bed materials should also be tested in the system to verify the difference in in-bed fuel conversion between using an inert bed material and an oxygen carrier at moderate/high bed temperatures. It would be especially interesting to study an oxygen carrier which has particularly high reactivity towards methane such as C28 (Mn-based perovskite oxygen carrier material, $CaMn_{0.775}Mg_{0.1}Ti_{0.125}O_{3-\delta}$). Additional OCAC experiments should be conducted with a fuel gas composition similar to what is expected in a PSA off-gas stream in an SMR production plant for hydrogen production. It would also be interesting to measure the NO_x in the OCAC reactor to investigate if a significant reduction in the NO_x emissions from the furnace can be expected for the proposed application in relation to the conventional process.

The results from the lab-scale experiments on the bed-to-tube heat transfer coefficient indicate that it should be interesting to perform follow-up experiments at high bed temperature at larger scale. This could be used to verify that high bed-to-tube heat transfer coefficients can be expected in a FBHE at high bed temperature at similar process conditions as in the proposed plant configurations. It would also be interesting to use vertical tubes, which is targeted for the proposed processes in this thesis.

The techno-economic assessment of the hydrogen production plant could be extended to also include SMR-CLC with natural gas as fuel, which has been evaluated previously by other authors[13, 15], as well as SMR-CLC with biomass as fuel which was presented in Paper I. This could provide a more complete overview of the possibilities to integrate fluidized beds as a heat source for SMR using different kinds of fuels as well as the possibility of inherent CO_2 capture.

Abbreviations

AFR	Air-fuel ratio
BEC	Bare Erected Cost
BFB	Bubbling fluidized bed
BIO	Biomass
BUA	Bottom-up approach
C28	Mn-based perovskite oxygen carrier material, $CaMn_{0.775}Mg_{0.1}Ti_{0.125}O_{3-\delta}$
CAGR	Compound annual growth rate
CEPCI	Chemical Engineering Plant Cost Index
CFB	Circulating fluidized bed
CCF	Capital charge factor
CLC	Chemical-looping combustion
COP21	2015 United Nations Climate Change Conference held in Paris
FBHE	Fluidized bed heat exchanger
FCEV	Fuel Cell Electric Vehicle
GFF	Gas-fired furnace
GHG	Greenhouse gas emissions
H_{bed}	Bed height
HX	Heat exchanger
HYBRIT	Joint venture aiming at substituting coal with hydrogen in steel production
LCOH	Levelized cost of hydrogen
LD slag	Steel converter slag from the Linz-Donawitz process
LHV	Lower heating value
O&M	Operations and maintenance
OCAC	Oxygen carrier aided combustion
MP	Measurement point
NDIR	Nondispersive infrared sensors
NG	Natural gas
PSA	Pressure swing adsorption
SMR	Steam methane reforming
SUCCESS	Research project aimed for scale-up of CLC
TPC	Total plant cost

Nomenclature

A_i	Tube inside surface area
A_o	Tube outside surface area
C	Equipment cost with the capacity S
C_o	Reference cost of equipment with reference capacity S_0
d_p	Weighted mean particle diameter based on sieving
E_{CO2}	Specific CO_2 emissions
δ	Degree of oxygen deficiency
e_p	Emissivity of particles
e_b	Emissivity of bed (= $0.5(1+e_p)$)
e_s	Emissivity of tube surface
ε	Voidage in fluidized bed
ε_{BFB}	Voidage in bubbling fluidized bed
ε_{fixed}	Voidage in fixed bed (assumed to be equal to 0.4)
h_i	Tube inside heat transfer coefficient
h_o	Bed-to-tube surface (or outside) heat transfer coefficient
h_{rad}	Radiative contribution to the outside heat transfer coefficient

h_w	Heat transfer coefficient through the tube wall
k_w	Thermal conductivity of tube wall
$\dot{m}$	Mass flow
$\dot{m}_{NG,eq}$	Equivalent flow of NG to the process including feed and supplementary fuel
$\dot{m}_{NG,tot}$	Total flow of NG to the process including feed and supplementary fuel
$\dot{M}$	Molar flow
n	Scale factor in economic calculations
$\eta_{el,ref}$	Efficiency of reference plant for electricity production
$\eta_{th,ref}$	Efficiency of reference plant for heat production
η_{H2}	Hydrogen production efficiency
η_{eq,H_2}	Equivalent hydrogen production efficiency
η'_{eq,H_2}	Equivalent hydrogen production efficiency based on that only electricity export is possible
P	Pressure
Q	Heat load delivered in FBHE experiment
Q_{th}	Heat delivered from steam export
ρ_b	Poured bulk density
ρ_g	Gas density
ρ_p	Particle density (= $\rho_b/(1-\varepsilon_{fixed})$)
S	Capacity (scaling parameter in cost functions)
S_o	Capacity for reference equipment
σ	Stefan Boltzmann constant (=5.67*10-8 W/(m^{2}K^4))
T_b	Bed temperature
T_{fg}	Reformer furnace flue gas temperature
$T_{furnace}$	Furnace temperature
$T_{s,i}$	Tube inside surface temperature (°C)
$T_{s,o}$	Tube outside surface temperature (°C)
T_{water}	Mean water temperature in the tube (°C)
u_{mf}	Minimum fluidization velocity
u_t	Terminal velocity
U	Overall heat transfer coefficient
W_{el}	Net electricity production
z	Number of units

References

[1] Smil V. Energy Transitions: Global and National Perspectives. & BP Statistical Review of World Energy. 2017.

[2] IPCC. Global Warming of 1.5°C. An IPCC Special Report on the impacts of global warming of 1.5°C above pre-industrial levels and related global greenhouse gas emission pathways, in the context of strengthening the global response to the threat of climate change, sustainable development, and efforts to eradicate poverty. World Meteorological Organization, Geneva, Switzerland. 2018. p. 32.

[3] Ogden JM. Hydrogen as an Energy Carrier: Outlook for 2010, 2030, and 2050. Institute of Transportation Studies University of California; 2004.

[4] IAEA. Hydrogen as an energy carrier and its production by nuclear power. 1999. p. 101.

[5] IEA. Technology Roadmap: Hydrogen and Fuel Cells. Paris, France, 2015.

[6] Liu K, Song C, Subramani V. Hydrogen and Syngas Production and Purification Technologies. Hoboken, New Jersey: John Wiley & Sons, Inc.; 2010.

[7] Ewan BCR, Allen RWK. A figure of merit assessment of the routes to hydrogen. International Journal of Hydrogen Energy. 2005;30:809-19.

[8] IEA. Closer look at the deployment of fuel cell EVs as of Dec. 2017. 2018.

[9] Driving Electric. Hyundai and Kia to build 500,000 hydrogen cars by 2030, https://www.drivingelectric.com/news/757/hyundai-and-kia-build-500000-hydrogen-cars-2030; 2018 [Accessed: 2019-04-13].

[10] HYBRIT. HYBRIT - Fossil-Free Steel: Summary of Findings from HYBRIT Pre-Feasibility Study 2016–2017. 2018.

[11] Stenberg V, Rydén M, Mattisson T, Lyngfelt A. Exploring novel hydrogen production processes by integration of steam methane reforming with chemical-looping combustion (CLC-SMR) and oxygen carrier aided combustion (OCAC-SMR). International Journal of Greenhouse Gas Control. 2018;74:28-39.

[12] IEAGHG. Techno-Economic Evaluation of SMR Based Standalone (Merchant) Plant with CCS. 2017.

[13] Rydén M, Lyngfelt A. Using steam reforming to produce hydrogen with carbon dioxide capture by chemical-looping combustion. International Journal of Hydrogen Energy. 2006;31:1271-83.

[14] Adánez J, Abad A, García-Labiano F, Gayán P, de Diego LF. Progress in Chemical-Looping Combustion and Reforming technologies. Progress in Energy and Combustion Science. 2012;38:215-82.

[15] Spallina V, Shams A, Battistella A, Gallucci F, Annaland MvS. Chemical Looping Technologies for H_2 Production With CO_2 Capture: Thermodynamic Assessment and Economic Comparison. Energy Procedia. 2017;114:419-28.

[16] Pans MA, Abad A, de Diego LF, García-Labiano F, Gayán P, Adánez J. Optimization of H_2 production with CO_2 capture by steam reforming of methane integrated with a chemical-looping combustion system. International Journal of Hydrogen Energy. 2013;38:11878-92.

[17] Abad A. Chemical looping for hydrogen production. In: Fennell P, Anthony, B., editor. Calcium and Chemical Looping Technology for Power Generation and Carbon Dioxide (CO_2) Capture. Cambridge, U.K: Woodhead Publishing; 2015. p. 327-67.

[18] Luo M, Yi Y, Wang S, Wang Z, Du M, Pan J, et al. Review of hydrogen production using chemical-looping technology. Renewable and Sustainable Energy Reviews. 2018;81:3186-214.

[19] Moud PH, Andersson KJ, Lanza R, Pettersson JBC, Engvall K. Effect of gas phase alkali species on tar reforming catalyst performance: Initial characterization and method development. Fuel. 2015;154:95-106.

[20] Alstrup I, Rostrup-Nielsen JR, Røen S. High temperature hydrogen sulfide chemisorption on nickel catalysts. Applied Catalysis. 1981;1:303-14.

[21] Wu H, La Parola V, Pantaleo G, Puleo F, Venezia A, Liotta L. Ni-Based Catalysts for Low Temperature Methane Steam Reforming: Recent Results on Ni-Au and Comparison with Other Bi-Metallic Systems. Catalysts. 2013;3:563-83.

[22] Rostrup-Nielsen J, Christiansen LJ. Concepts in Syngas Manufacture. London: Imperial College Press; 2011.

[23] DOE/NETL. Assessment of Hydrogen Production with CO_2 Capture, Volume 1: Baseline State-of-the-Art Plants. DOE/NETL-2010/1434. 2010.

[24] Carlsson M. Carbon Formation in Steam Reforming and Effect of Potassium Promotion. Johnson Matthey Technology Review. 2015;59:313-8.

[25] Boot-Handford ME, Abanades JC, Anthony EJ, Blunt MJ, Brandani S, Mac Dowell N, et al. Carbon capture and storage update. Energy & Environmental Science. 2014;7:130-89.

[26] Li J, Zhang H, Gao Z, Fu J, Ao W, Dai J. CO_2 Capture with Chemical Looping Combustion of Gaseous Fuels: An Overview. Energy & Fuels. 2017;31:3475-524.

[27] Lyngfelt A, Linderholm C. Chemical-Looping Combustion of Solid Fuels – Status and Recent Progress. Energy Procedia. 2017;114:371-86.

[28] Thunman H, Lind F, Breitholtz C, Berguerand N, Seemann M. Using an oxygen-carrier as bed material for combustion of biomass in a 12-MW_{th} circulating fluidized-bed boiler. Fuel. 2013;113:300-9.

[29] Rydén M, Hanning M, Corcoran A, Lind F. Oxygen Carrier Aided Combustion (OCAC) of Wood Chips in a Semi-Commercial Circulating Fluidized Bed Boiler Using Manganese Ore as Bed Material. Applied Sciences. 2016;6:347.

[30] Källén M, Rydén M, Lind F. Improved Performance in Fluidised Bed Combustion by the Use of Manganese Ore as Active Bed Material. 22nd International Conference on Fluidized Bed Combustion. Turku, Finland. 2015.

[31] Hallberg P, Hanning M, Rydén M, Mattisson T, Lyngfelt A. Investigation of a calcium manganite as oxygen carrier during 99h of operation of chemical-looping combustion in a $10kW_{th}$ reactor unit. International Journal of Greenhouse Gas Control. 2016;53:222-9.

[32] Rydén M, Jing D, Källén M, Leion H, Lyngfelt A, Mattisson T. CuO-Based Oxygen-Carrier Particles for Chemical-Looping with Oxygen Uncoupling – Experiments in Batch Reactor and in Continuous Operation. Industrial & Engineering Chemistry Research. 2014;53:6255-67.

[33] Hallberg P, Källen M, Jing D, Snijkers F, van Noyen J, Rydén M, et al. Experimental Investigation of $CaMnO_{3-\delta}$ Based Oxygen Carriers Used in Continuous Chemical-Looping Combustion. International Journal of Chemical Engineering. 2014:9.

[34] Källén M, Rydén M, Dueso C, Mattisson T, Lyngfelt A. $CaMn_{0.9}Mg_{0.1}O_{3-\delta}$ as Oxygen Carrier in a Gas-Fired 10 kW_{th} Chemical-Looping Combustion Unit. Industrial & Engineering Chemistry Research. 2013;52:6923-32.

[35] Hallberg P, Jing D, Rydén M, Mattisson T, Lyngfelt A. Chemical Looping Combustion and Chemical Looping with Oxygen Uncoupling Experiments in a Batch Reactor Using Spray-Dried $CaMn_{1-x}MxO_{3-\delta}$ (M = Ti, Fe, Mg) Particles as Oxygen Carriers. Energy & Fuels. 2013;27:1473-81.

[36] Gayán P, Pans MA, Ortiz M, Abad A, de Diego LF, García-Labiano F, et al. Testing of a highly reactive impregnated Fe_2O_3/Al_2O_3 oxygen carrier for a SR–CLC system in a continuous CLC unit. Fuel Processing Technology. 2012;96:37-47.

[37] Rydén M, Lyngfelt A, Mattisson T. $CaMn_{0.875}Ti_{0.125}O_3$ as oxygen carrier for chemical-looping combustion with oxygen uncoupling (CLOU)—Experiments in a continuously operating fluidized-bed reactor system. International Journal of Greenhouse Gas Control. 2011;5:356-66.

[38] Abad A, Adánez J, García-Labiano F, de Diego LF, Gayán P. Modeling of the chemical-looping combustion of methane using a Cu-based oxygen-carrier. Combustion and Flame. 2010;157:602-15.

[39] Chadeesingh DR, Hayhurst AN. The combustion of a fuel-rich mixture of methane and air in a bubbling fluidised bed of silica sand at 700°C and also with particles of Fe_2O_3 or Fe present. Fuel. 2014;127:169-77.

[40] Rydén M, Hanning M, Lind F. Oxygen Carrier Aided Combustion (OCAC) of Wood Chips in a 12 MW_{th} Circulating Fluidized Bed Boiler Using Steel Converter Slag as Bed Material. Applied Sciences. 2018;8:2657.

[41] Leion H, Mattisson T, Lyngfelt A. Use of Ores and Industrial Products As Oxygen Carriers in Chemical-Looping Combustion. Energy & Fuels. 2009;23:2307–15.

[42] Ortiz M, Gayán P, de Diego LF, García-Labiano F, Abad A, Pans MA, et al. Hydrogen production with CO_2 capture by coupling steam reforming of methane and chemical-looping combustion: Use of an iron-based waste product as oxygen carrier burning a PSA tail gas. Journal of Power Sources. 2011;196:4370-81.

[43] Kunii D, Levenspiel O. Fluidization Engineering (2nd edition). Boston: Butterworth-Heinemann; 1991.

[44] Leckner B. Fluidized Bed Reactors: Heat and Mass Transfer. In: Michaelides E, Crowe CT, Schwarzkopf JD, editors. Multiphase Flow Handbook (second edition): CRC Press; 2017. p. 994-1029.

[45] Zhu Q. Developments in circulating fluidised bed combustion. In: Centre ICC, editor.2013.

[46] Mickley HS, Fairbanks DF. Mechanism of heat transfer to fluidized beds. AIChE Journal. 1955;1:374-84.

[47] Grewal NS, Saxena SC. Heat transfer between a horizontal tube and a gas-solid fluidized bed. International Journal of Heat and Mass Transfer. 1980;23:1505-19.

[48] Andeen BR, Glicksman LR. Heat transfer to horisontal tubes in shallow fluidized beds. ASME-AIChe Heat Transfer Conference. St Louis, MO, 1976.

[49] Genetti WE, Schmall RA, Grimmett ES. The Effect of Tube Orientation on Heat Transfer With Bare and Finned Tubes in a Fluidized Bed. Chem Engr Progr Sym Ser. 1971;116:90-6.

[50] Ainshtein VA. "An Investigation of Heat Transfer Process Between Fluidized Beds and Single Tubes Submerged in the Bed" in Zabordsky, SS., "Hydrodynamics and Heat Transfer in Fluidized Beds" MIT Press. Cambridge, Massachusetts, 1966.

[51] Gelperin, NI, Kruglikov, V, Ya., and Ainshtein, VG., in Ainshtein, VG., and Gelperin, NI., "Heat Transfer between a Fluidized Bed and a Surface," Inter Chem Engrg. 1966;6.

[52] Vreedenberg HA. Heat transfer between a fluidized bed and a horizontal tube. Chem Eng Sci,. 1958;9:52-60.

[53] Corcoran A, Knutsson P, Lind F, Thunman H. Comparing the structural development of sand and rock ilmenite during long-term exposure in a biomass fired 12MW$_{th}$ CFB-boiler. Fuel Processing Technology. 2018;171:39-44.

[54] Berdugo Vilches T, Lind F, Rydén M, Thunman H. Experience of more than 1000h of operation with oxygen carriers and solid biomass at large scale. Applied Energy. 2017;190:1174-83.

[55] Lyngfelt A, Mattisson T, Rydén M, Linderholm C. 10,000 h of Chemical-Looping Combustion Operation – Where Are We and Where Do We Want to Go? 5th International Conference on Chemical Looping. Park City, Utah, USA, 2018.

[56] Moldenhauer P, Linderholm C, Rydén M, Lyngfelt A. Experimental investigation of chemical-looping combustion and chemical-looping gasification of biomass-based fuels using steel converter slag as oxygen carrier. International Conference on Negative CO_2 Emissions. Gothenburg, Sweden, 2018.

[57] Martínez I, Romano MC, Chiesa P, Grasa G, Murillo R. Hydrogen production through sorption enhanced steam reforming of natural gas: Thermodynamic plant assessment. International Journal of Hydrogen Energy. 2013;38:15180-99.

[58] Turton R, Bailie RC, Whiting WB, Shaeiwitz JA. Analysis, Synthesis and Design of Chemical Processes (3rd edition), 2009.

[59] Otmar Bertsch, Bertsch Energy GmbH & Co KG. Personal communication. 2018.

[60] Roberts RD, Brightling J. Maximize tube life by using internal and external inspection devices. Process Safety Progress. 2005;24:258-65.

[61] Incropera F, Dewitt D, Bergman T, Lavine A. Principles of heat and mass transfer. 7th ed. ed. Singapore, 2013.

[62] Stenberg V, Sköldberg V, Öhrby L, Rydén M. Evaluation of bed-to-tube surface heat transfer coefficient for a horizontal tube in bubbling fluidized bed at high temperature. Powder Technology. 2019.

[63] Special Metals Corporation. High Performance Alloys Literature - Inconel alloy 600. 2008.

[64] Andersson B-Å. Heat transfer in stationary fluidized bed boilers. Gothenburg, Sweden: Chalmers University of Technology; 1988.